NMM2008, Okinawa

Development and Application of Magneto-Optical Microscope Using Polarization-Modulation Technique

K. Sato (Tokyo Univ. Agric. & Tech/JST)
T. Ishibashi (Nagaoka Univ. Technology)

Outline

1. Introduction
2. MO imaging using polarization modulation technique
3. MO indicator film
   Bi:YIG by MOD method
4. Magnetic imaging
   1. Patterned MgB_2 film
   2. Magnetic nanostructures
5. Summary

1. Introduction

Magnetic Imaging using MO method

- Magneto-optical (MO) microscopes have been used as one of the most significant techniques for an observation of magnetic domain structures in magnetic materials.
- Recently, this technique attracts great attention as a powerful tool for visualization of invisible phenomena: e.g.,
  - spin-accumulation in nonmagnetic semiconductors (1,2)
  - magnetic flux intrusion in superconductors (3)-(5) .

(1) S. A. Crooker et al.: Science, Vol.309, pp.2191-2195 (2005).
(2) M. Yamanouchiet al.: Lett. Nature, Vol.428, pp.539-542 (2004).
(3) S. Gotoh et al.: Jpn. J. Appl. Phys., Vo.29, L1083-L1085 (1990).
(4) M. V. Indenbom et al.: Physica C, Vol.166, pp.486-496 (1990).
(5) P.E. Goa et al.: Rev. Sci. Instrum., Vol.74, pp. 141-146 (2003).

Magnetic Imaging of stray magnetic field using MO method

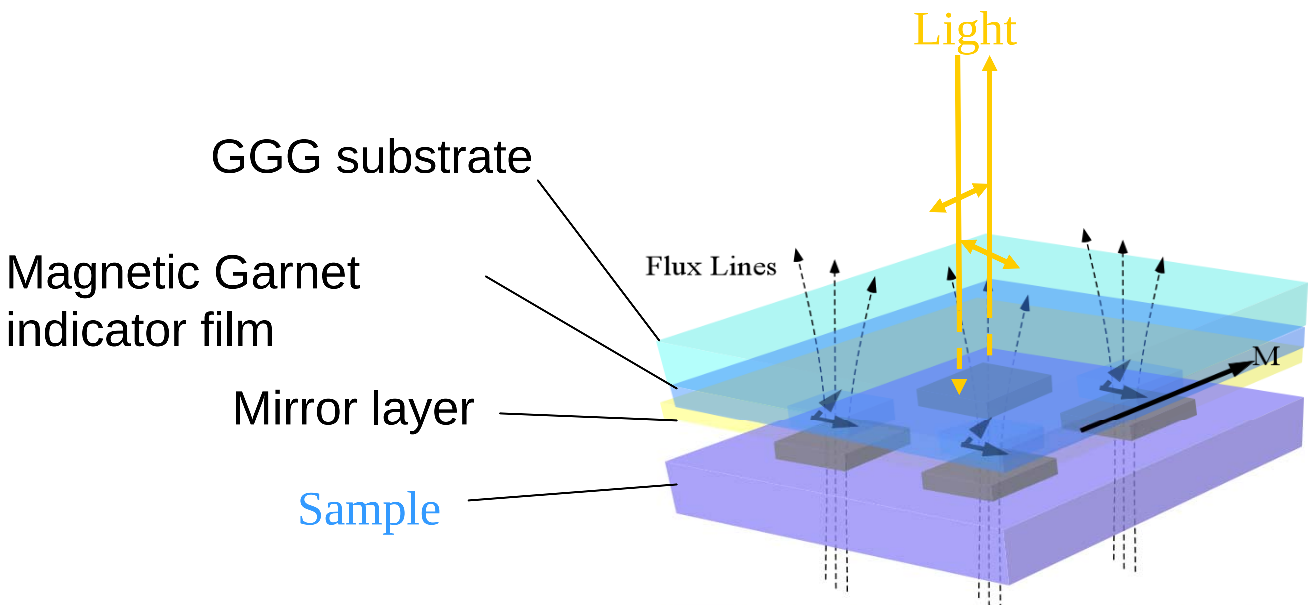

Stray field from sample magnetize the garnet film locally, and the distribution of field can be detected by means of MO method, as a polarization image.

Example of Magnetic imaging using MO method

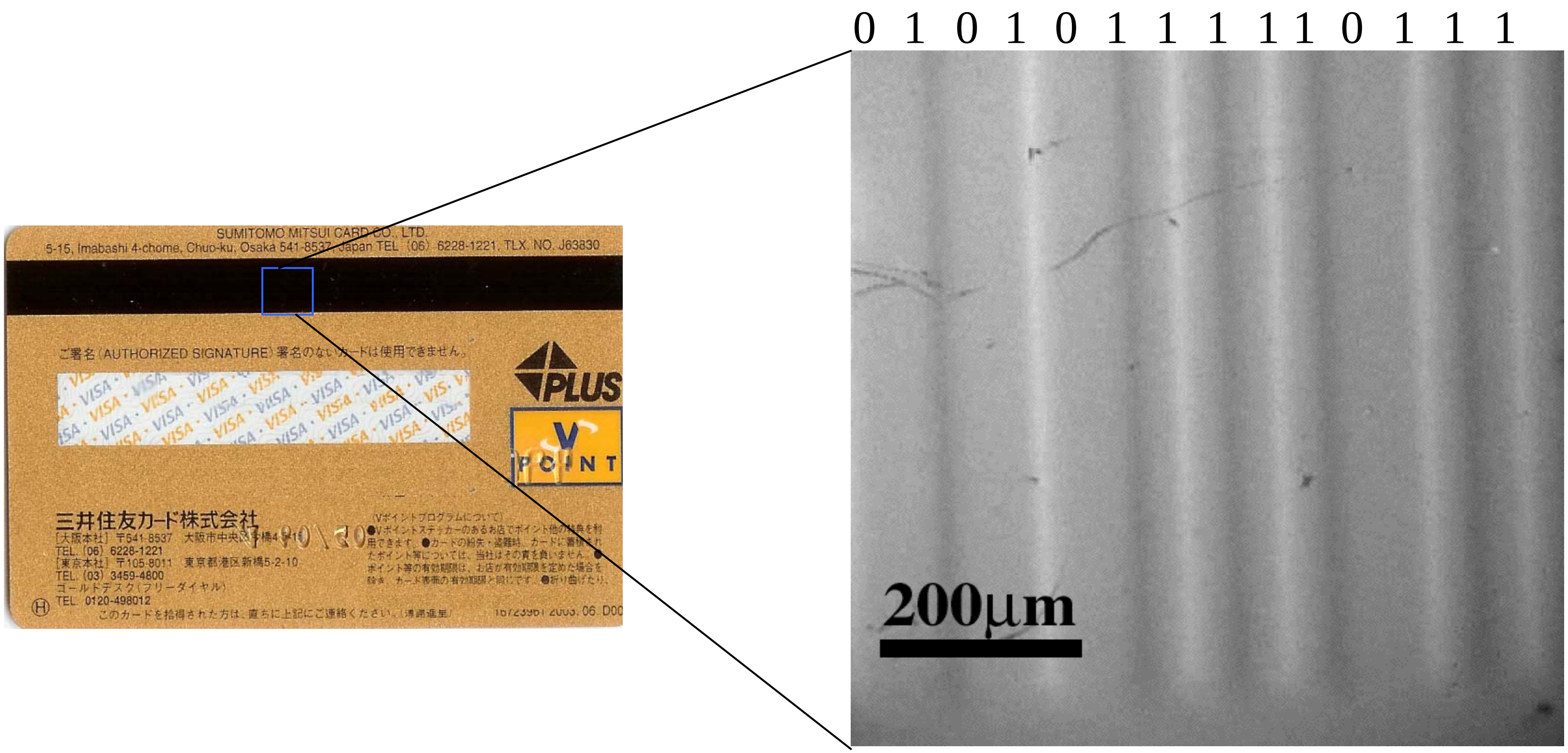

Advantages of MO imaging to other imaging techniques

- MO microscopes have technical advantages:
  - a short measuring time
  - a simple instrumental setup compared with other imaging techniques, e.g., a magnetic force microscope (MFM) (6), a superconducting quantum interference device (SQUID) microscope (7) and a Hall-probe microscope (8).

Magnetic Imaging

	Quantitative Magnteic measurement	Spatial Resolution	Dynamic measurement	Measuring time for one image	Special sample treatment
Scanning SQUID microscope	○:10^{-7}T	> 1 μm	no	> 1 min	no
Scanning Tunneling Microscope (STM)	×	< 1 nm	no	> 1 min	Surface treatment (cleavage, etc.)
Magnetic Force Microscope (MFM)	△	< 10 nm	no	> 1 min	no
Bitter Method	×	< 10 nm	no	～10 msec	Deposition of magnetic materials
Lorenz Microscope	○	< 1 μm	yes	～10 msec	Thinner the sample for TEM measurement
Magneto-Optical Microscope	○:10^{-5}T	< 1 μm	yes	～10 msec	no

MO microscope has advantages shown above.
In addition, it is easy to develop it with low temperature, magnetic field, etc, since the MO microscope is a simple technique based on optical microscope.

Conventional MO microscope

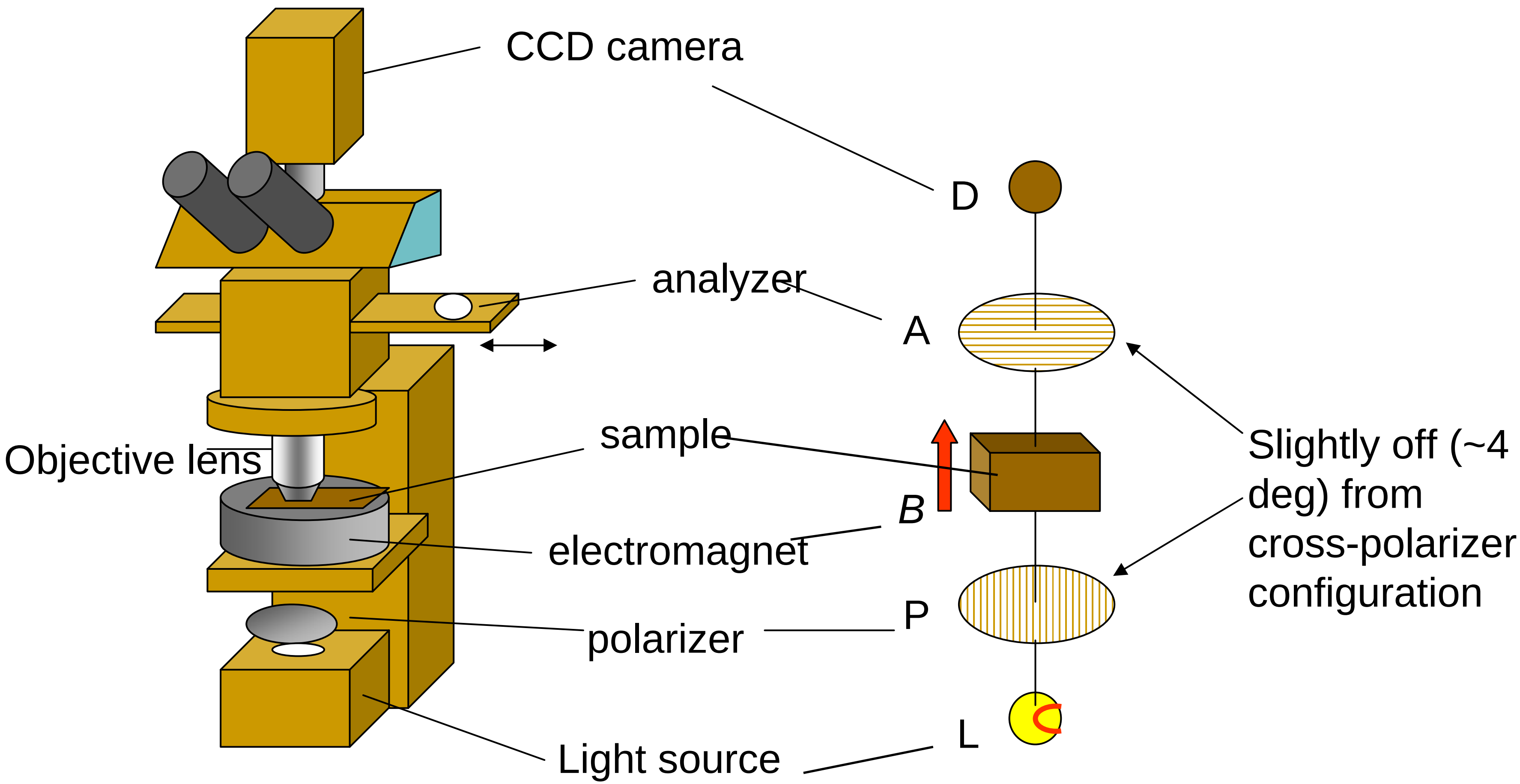

MO observation using cross-polarizer technique

- Light intensity is symmetrical for plus and minus magnetic field direction, so that no magnetic contrast can be observed.
- Angle between two polarizers should be slightly off (~4°) from 90 ° in order to get a contrast.

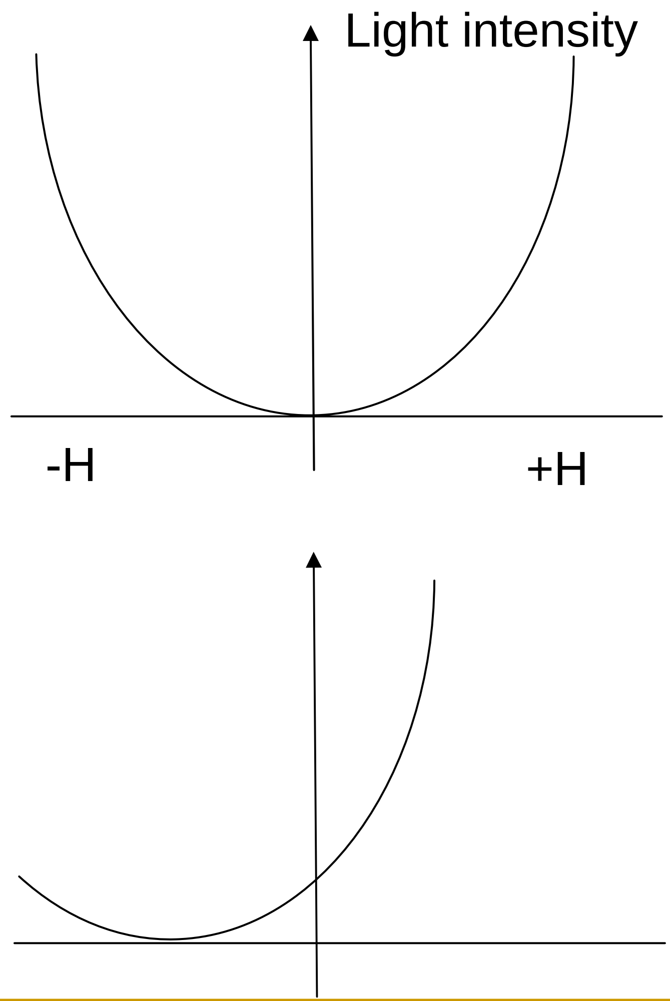

Problems in MO imaging

- Image is dark. Quantitative measurement of MO values, Faraday effect, Kerr effect in inhomogeneous samples is difficult.

  ↳ MO microscope using polarization modulation technique.

- Zigzag Domain structure in MO indicator film deteriorates images.

  ↳ Bi:YIG prepared by metal-organic decomposition method.

2. MO microscope using polarization modulation method

Polarization modulation technique using photoelastic modulator (PEM)

- Magneto-optical spectra have been measured using PEM which modulates retardation of light at *p* rad/s to produce LP, LCP and RCP sequentially.
- Polarization rotation is given by detecting 2p component and ellipticity is given by p component.

Retardation modulation using PEM

- P and A are linear polarizers, M photoelastic modulator(PEM), D a detector.
- PEM consists of an isotropic transparent material (quartz, CaF_2 etc.) and a piezoelectric vibrator made of quartz.
- If PEM is fed with HF electric field with angular frequency of p [rad/s] , standing wave of the acoustic sound which generates in the transparent material uniaxial anisotropy oscillating with angular frequency p [rad/s, which in turn leads to appearance of Δn.
- Optical retardation $\delta = \Delta nl/\lambda$ is modulated with an angular frequency of p [rad/s], therefore

$$\delta = \delta_0 \sin pt \ .$$

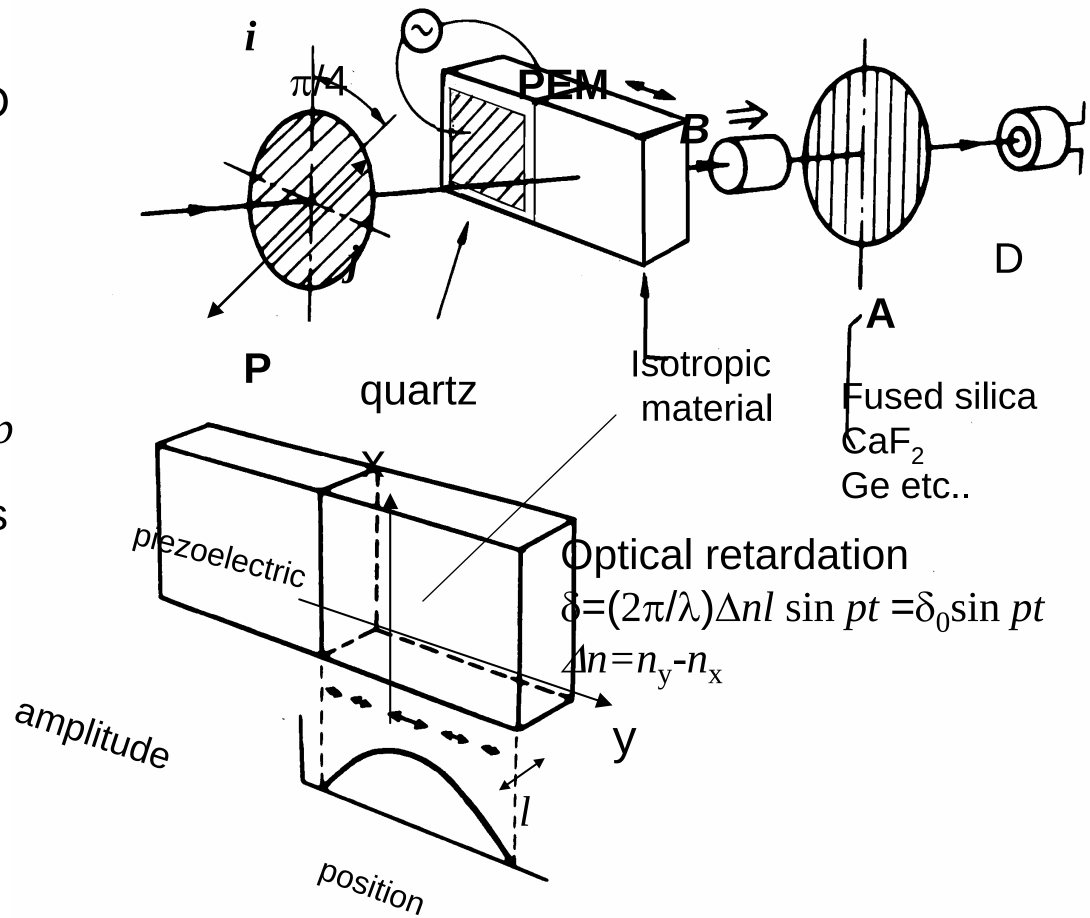

Scematic explanation of retardation modulation

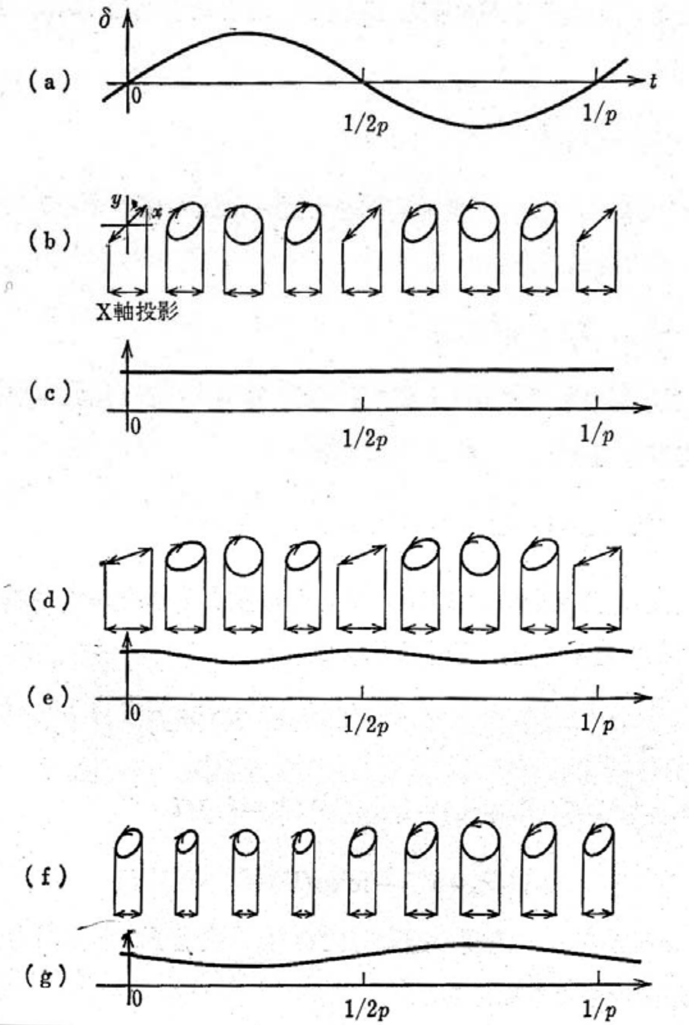

- Fig.(a) shows time-variation of optical retardation δ If the amplitude δ_0 takes a value π/2, positive and negative peaks of δ correspond to RCP (right circularly polarized light) and LCP (left circularly polarized light), respectively.
- If the sample shows neither rotation nor circular dichroism, the lotus of the detected electric field vector changes as LP-RCP-LP-LCP-LP, as shown in Fig.(b). The x-component does not change as shown in Fig. (c).
- If the sample show rotation, the lotus varies as shown in Fig. (d) and the x-component oscillates with angular frequency of 2p as illustrated in Fig.(e).
- If circular dichroism exists vector length of RCP and LCP becomes different as shown in Fig. (f), leading to oscillation of x-component with angular frequency of *p*[rad/s].

MO Spectrometer layout

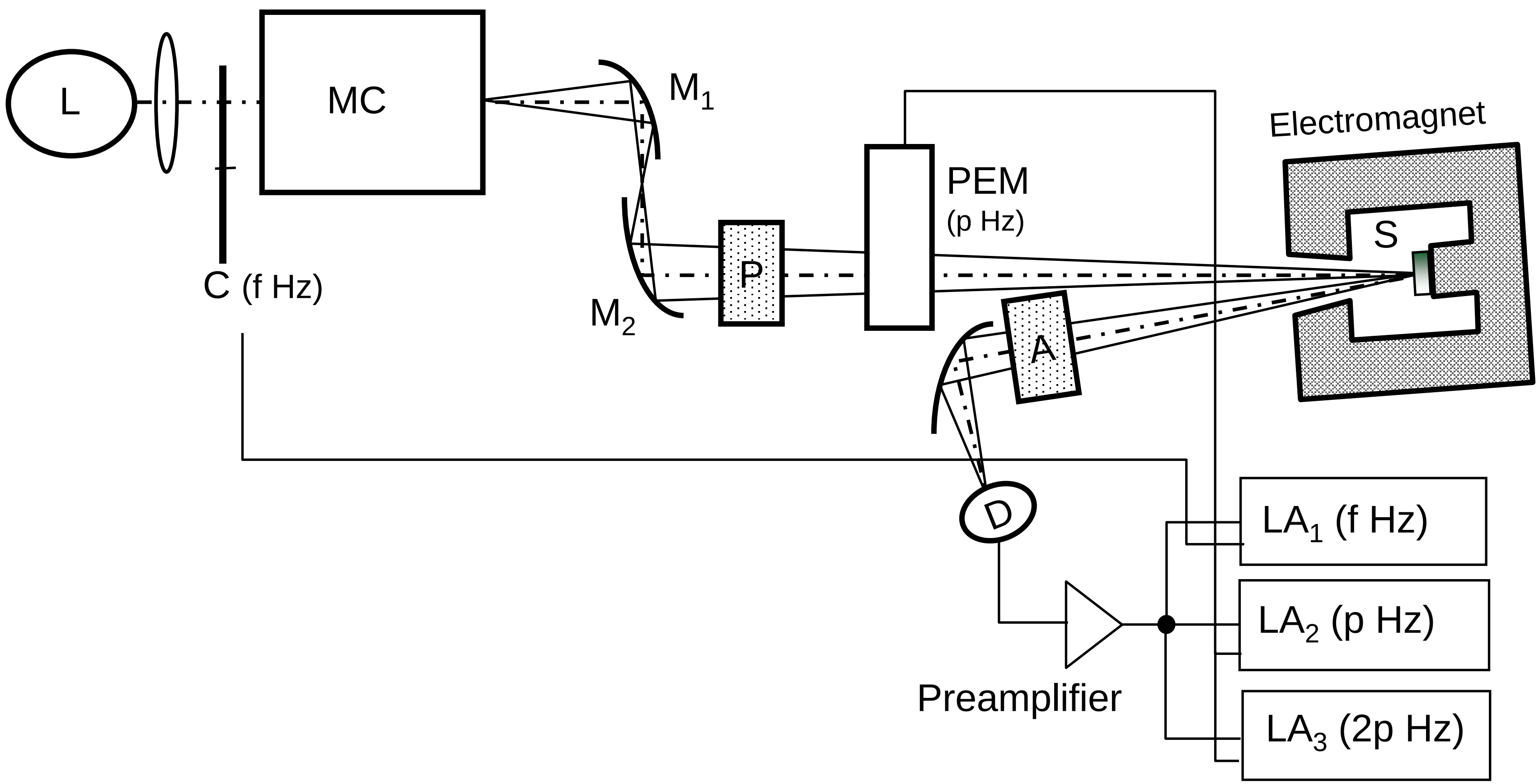

Magneto-optical spectrometer

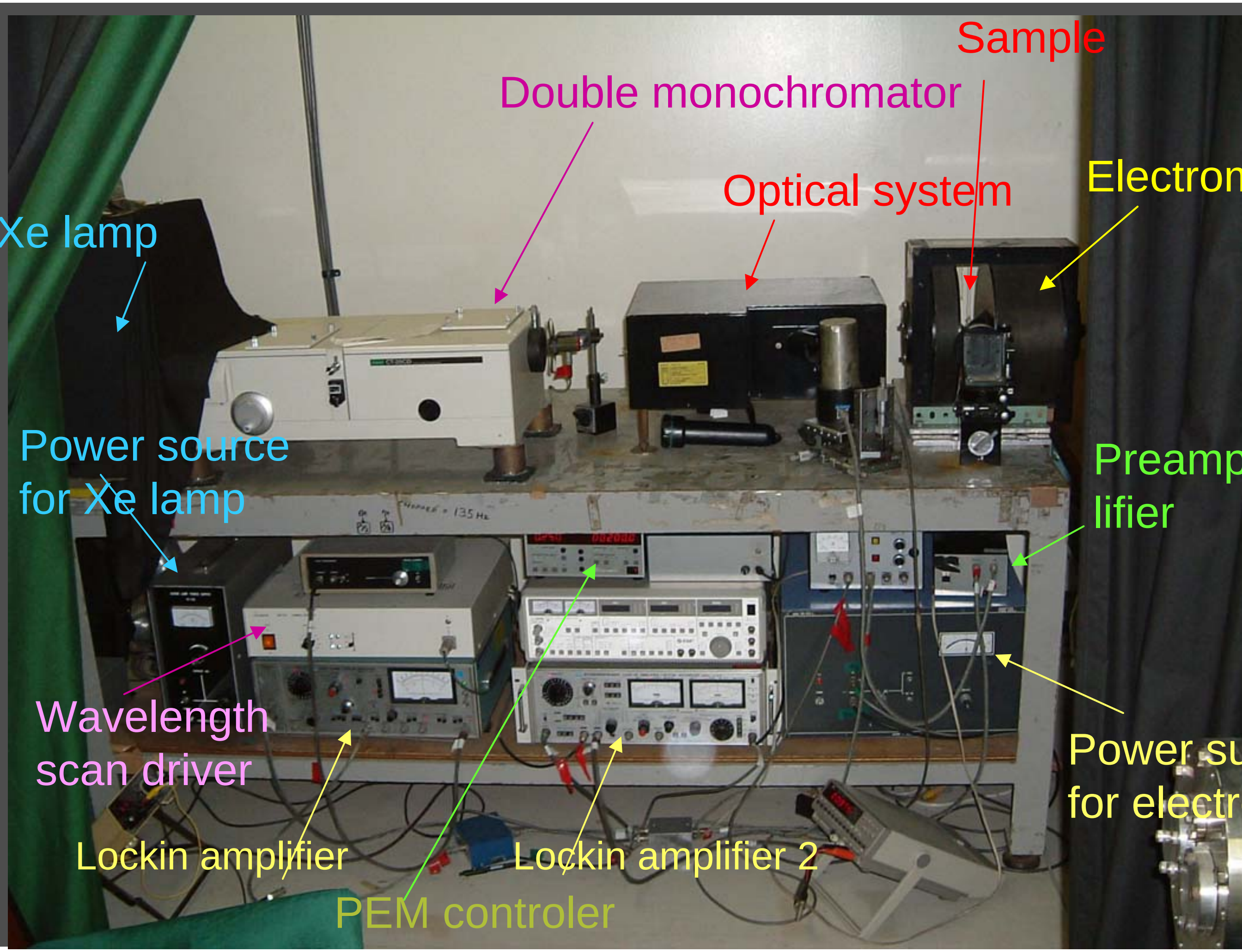

How to apply modulation technique to MO microscopy

- Conventional PEM employs a modulation frequency as high as 50 KHz, which exceeds the frame rate of CCD cameras and cannot be directly applicable to MO microscopy.
- In the retardation modulation technique, rotation produces difference in x-component of linear polarization (LP) and circular polarization (CP), while circular dichroism (=ellipticity) produces difference in the x-component of right circular and left circular polarizations

Rotation produces difference between LP and CP

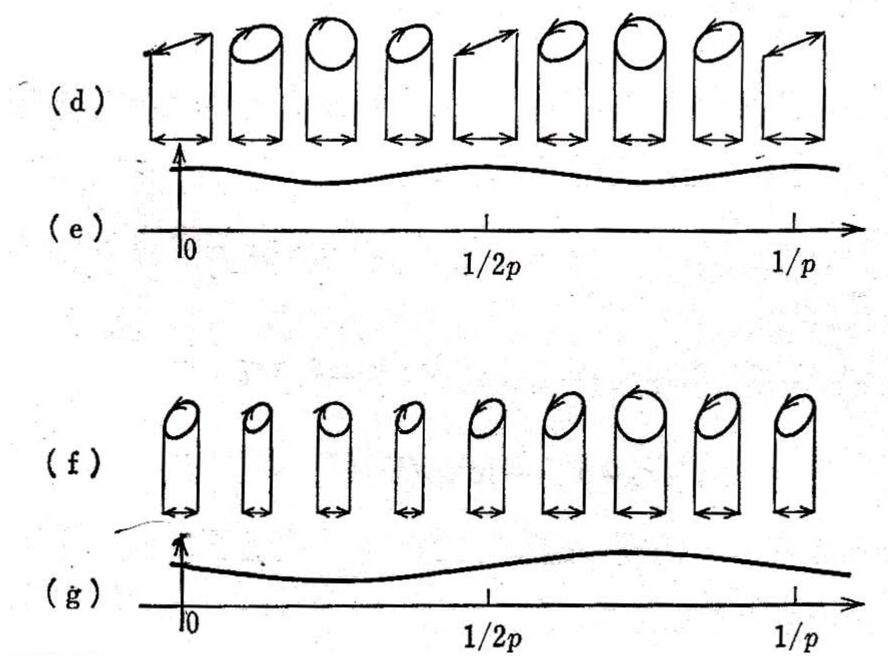

Circular dichroism produces difference between RCP and LCP

Modulation technique using image processing

- It is thus elucidated as follows:
- MO rotation image can be obtained by an image processing to take difference between LP and CP images.
- MO ellipticity image can be obtained by an image processing to take difference between RCP and LCP images.

Novel MO microscope with retardation modulation

Microscope: Olympus BH-UMA
CCD camera:Hamamatsu C4880 (Cooled)
Analyzer(fixed): Glan-Thomson MG*B10
Objective lens: NeoSPlanNIC 10 × 50
Rotatable quarter waveplate:ACP-400-700
(acromatic waveplate)
Polarizer(fixed):Glan-Thomson (MG*B10)
Bandpass filter: Interference filter
(450, 500,550, 600, 650 nm, BW=10nm)
Light source: Halogen-tungsten lamp 20W

Principle of image processing

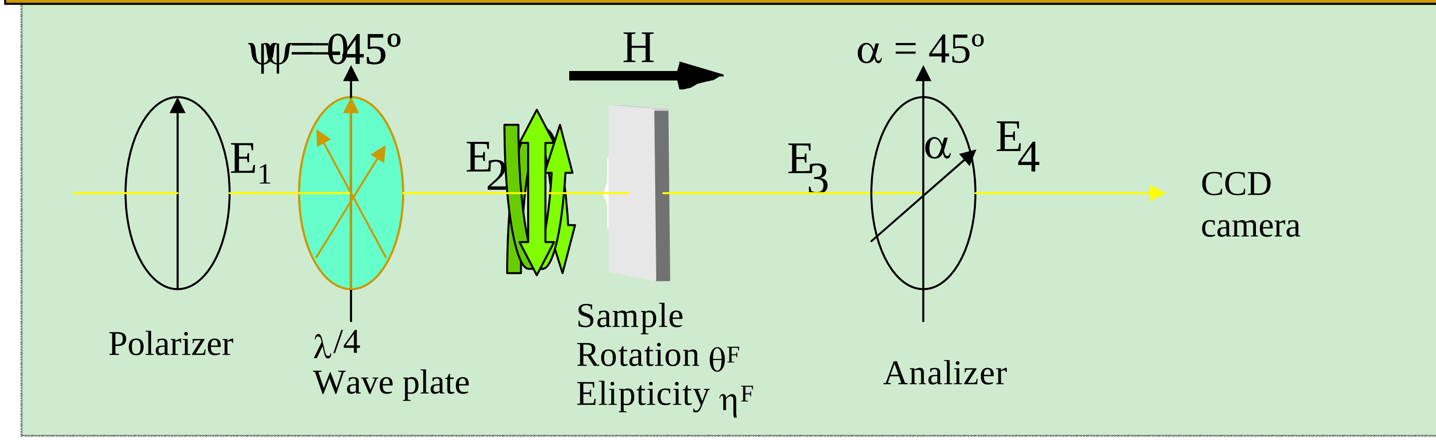

ψ= 0º LP
45º RCP
-45 º LCP

$$\mathbf{E}_2 = \mathbf{ASQPE}_1$$

$$= \frac{1}{2}\begin{pmatrix} 1 & 1 \\ 1 & 1 \end{pmatrix}\begin{pmatrix} \cos\theta_F + i\eta_F \sin\theta_F & -\sin\theta_F + i\eta_F\cos\theta_F \\ \sin\theta_F - i\eta_F\cos\theta_F & \cos\theta_F + i\eta_F\sin\theta_F \end{pmatrix}\begin{pmatrix} 1+i\cos 2\varphi & i\sin 2\varphi \\ i\sin 2\varphi & 1-i\cos 2\varphi \end{pmatrix}\begin{pmatrix} 1 & 0 \\ 0 & 0 \end{pmatrix}\begin{pmatrix} E_x \\ E_y \end{pmatrix}$$

$$= \frac{1}{2}\begin{pmatrix} \cos\theta_F + \sin\theta_F - \eta_F\left(\sin(2\varphi+\theta_F) - \cos(2\varphi+\theta_F)\right) + i\left\{\cos(2\varphi+\theta_F) + \sin(2\varphi+\theta_F) + \eta_F\left(\sin\theta_F - \cos\theta_F\right)\right\} \\ \cos\theta_F + \sin\theta_F - \eta_F\left(\sin(2\varphi+\theta_F) - \cos(2\varphi+\theta_F)\right) + i\left\{\cos(2\varphi+\theta_F) + \sin(2\varphi+\theta_F) + \eta_F\left(\sin\theta_F - \cos\theta_F\right)\right\} \end{pmatrix} E_x$$

$$I(\varphi) = \left(\cos\theta_F + \sin\theta_F - \eta_F\left(\sin(2\varphi+\theta_F) - \cos(2\varphi+\theta_F)\right)\right)^2$$

$$+ \left(\cos(2\varphi+\theta_F) + \sin(2\varphi+\theta_F) + \eta_F\left(\sin\theta_F - \cos\theta_F\right)\right)^2 \left|E_x\right|^2 / 4$$

$I(0^{\circ})$

$I(45^{\circ})$

$I(-45^{\circ})$

MO imaging using rotatable quarter waveplate as polarization modulator

Faraday rotation

$$\theta_F = \frac{1}{2}\sin^{-1}\left\{\frac{2I_{LP} - \left(I_{LCP} + I_{RCP}\right)}{\left(1-\eta_F{}^2\right)\left|E_x\right|^2}\right\}$$

$$\theta_F \approx \frac{1}{2}\left\{\frac{2I_{LP} - \left(I_{RCP} + I_{LCP}\right)}{\left(1-\eta_F{}^2\right)\left(I_{RCP} + I_{LCP}\right)}\right\}$$

Faraday ellipticity

$$\eta_F = \frac{1}{2}\left(I_{LCP} - I_{RCP}\right)/\left|E_x\right|^2$$

$$\eta_F \approx \frac{1}{2}\left(\frac{I_{LCP} - I_{RCP}}{I_{LCP} + I_{RCP}}\right)$$

T Ishibashi et al., J. Magn. Soc. Jpn. **4**, 278 (2004).
T Ishibashi et al., J. Appl. Phys. **100**, 093903 (2006).

Evaluation of Faraday rotation

Faraday rotation

$$\theta_F = \frac{1}{2}\sin^{-1}\left\{-\frac{2I(0)-\{I(\pi/4)+I(-\pi/4)\}}{(1-\eta_F{}^2)|E_x|^2}\right\}$$

$$\theta_F \approx \frac{1}{2}\left\{\frac{2I(0)-[I(\pi/4)+I(-\pi/4)]}{(1-\eta_F{}^2)[I(\pi/4)+I(-\pi/4)]}\right\}$$

Faraday ellipticity

$$\eta_F = -\frac{1}{2}\{I(\pi/4)-I(-\pi/4)\}/|E_x|^2$$

$$\eta_F \approx -\frac{1}{2}\left\{\frac{I(\pi/4)-I(-\pi/4)}{I(\pi/4)+I(-\pi/4)}\right\}$$

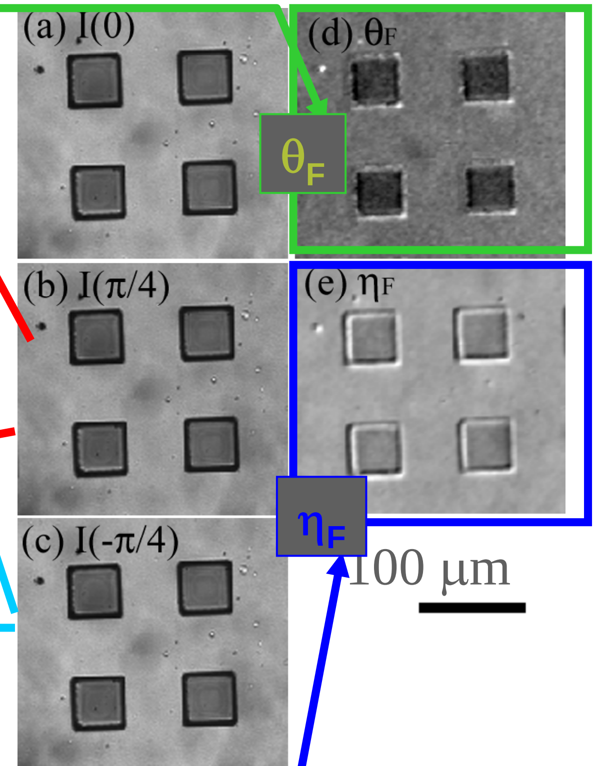

CCD image (a) *LP*, (b) *RCP*, (c) *LCP*,
Processed image (d) rotation (e) ellipticity

Sample

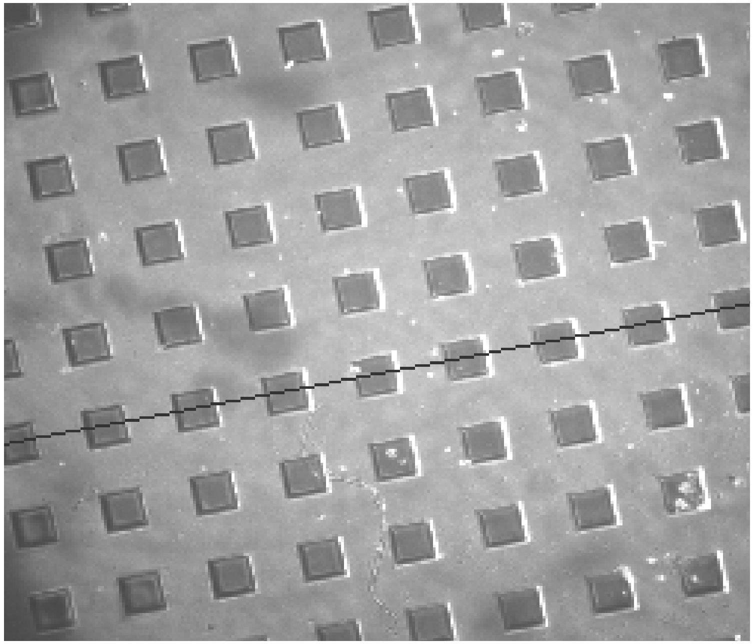

An optical microscope image

$Y_2BiFe_4GaO_{12}$ Film/glass sub.
prepared by MOD method
T. Ishibashi et al, J. Appl. Phys., 97, 013516 (2005).

Rectangular Dots array
Size 50μm×50μm
Thickness 200nm

Transmittances of glass substrate and garnet dot are quite different.
It is hard to obtain quantitative magnetic contrast by conventional MO imaging technique.

Image of Faraday Rotation

Magnetic field reversal.

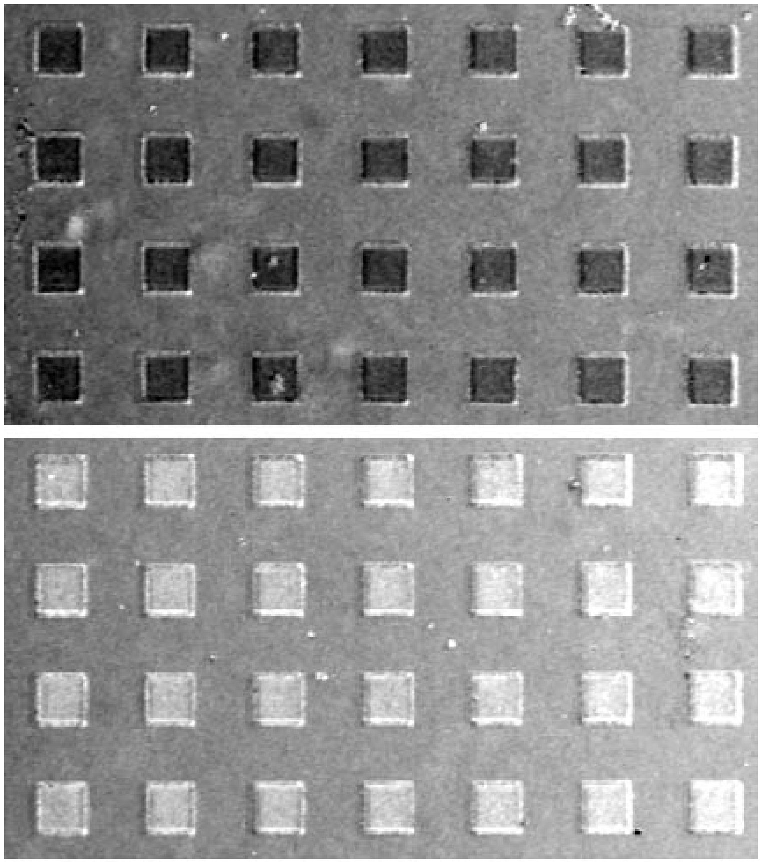

Image of Faraday ellipticity

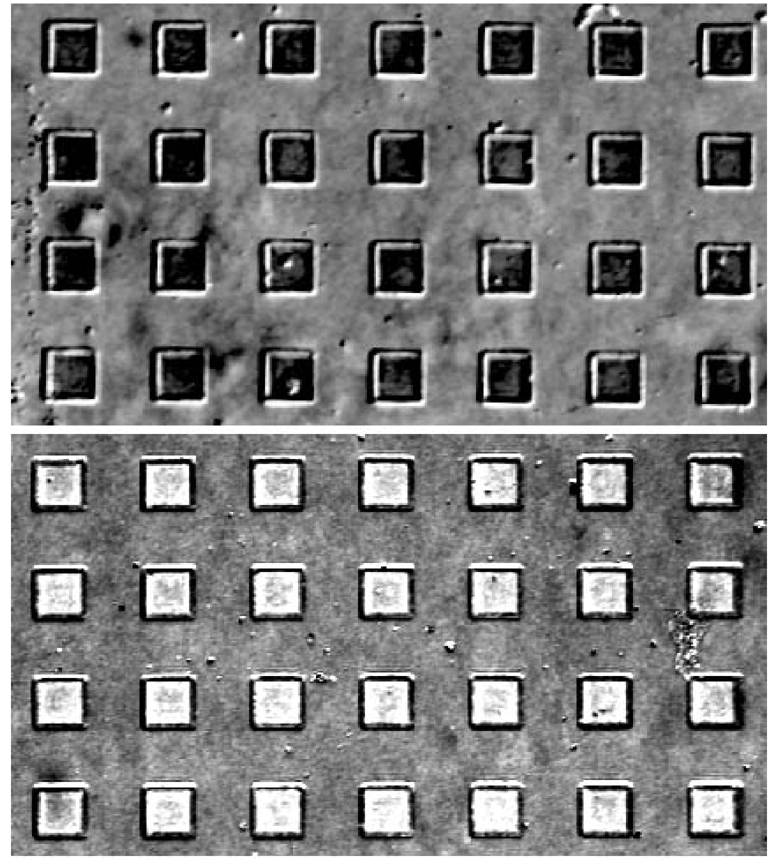

λ=500 nm

Reversal of magnetic contrast corresponding to magnetization reversal

Quantitative evaluation.

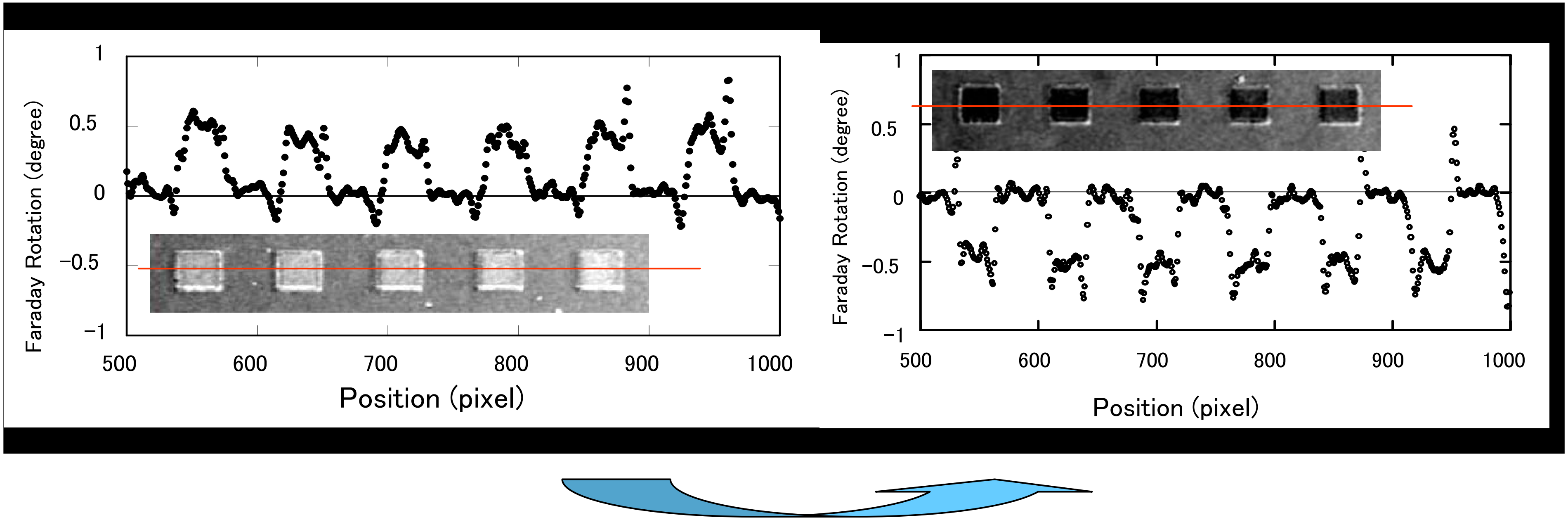

λ=500 nm

Rotation angle is obtained quantitatively.

Hysteresis measurement

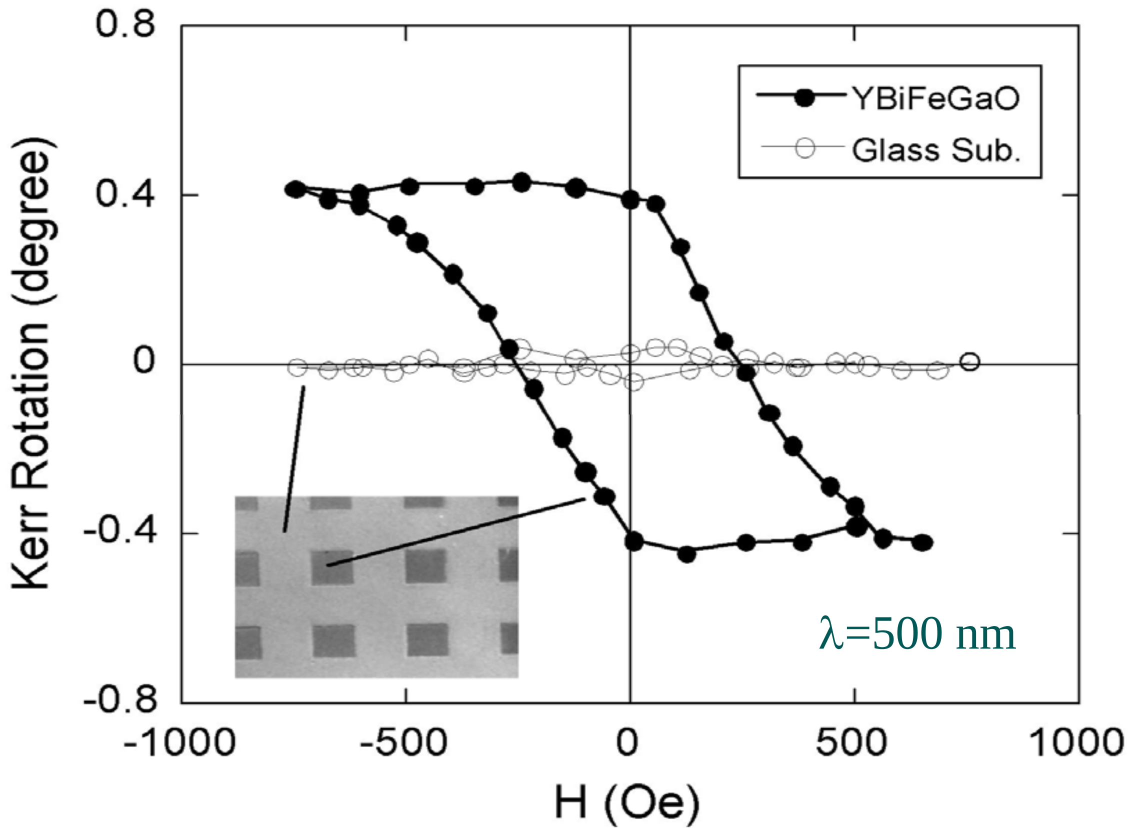

Magnetic field dependences of patterned garnet film measured with wavelength of 500 nm. Clear hysteresis loop was observed at garnet dot although no signal was obtained at glass substrate. Hysteresis data can be obtained for each pixels.

Averaging and smoothing

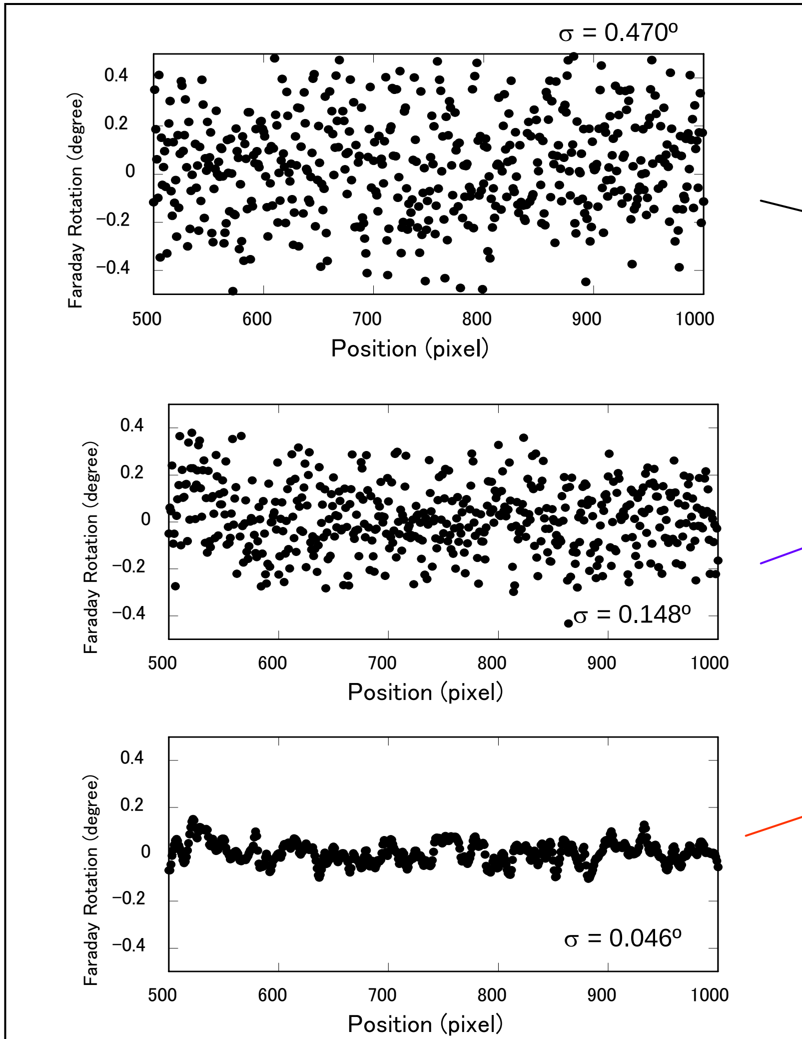

σ : standard deviation

1 shot

σ=0.920º

10 times accumulation

σ= 0.148º

10 times accumulation

+ smoothing

σ= 0.048º

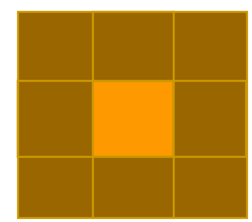

Faraday rotation and Faraday ellipticity spectra of patterned garnet film using MO microscope

Faraday rotation

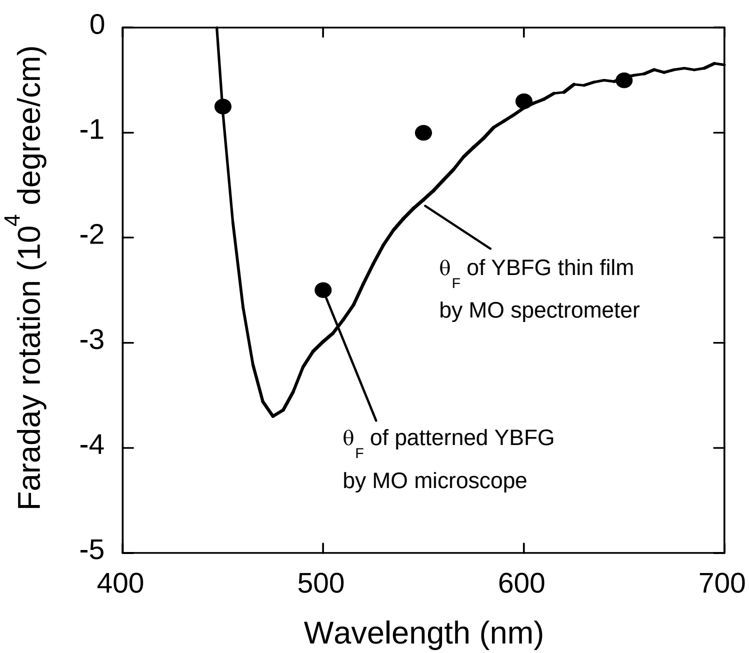

Faraday ellipticity

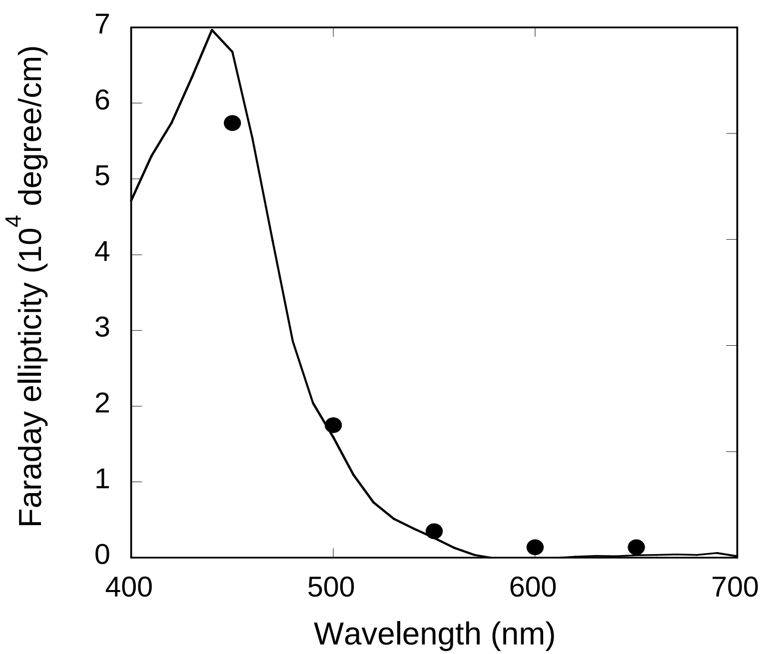

Dots show data measured by MO microscope using interference filter (450, 500,550, 600, 650 nm) with band width of 10nm. **Solid lines** show spectra measured by MO spectrometer for garnet film without pattering.

The merits of the method

- Merits
  - Simultaneous measurement of rotation and ellipticity in one cycle of measurement
  - Quantitative evaluation of rotation and ellipticity is possible (standard sample is not necessary)
  - Faraday image can be clearly displayed even in the sample with inhomogeneous transmission
  - Magnetic hysteresis loops at any pixel point can be displayed, once MO images are acquired for a sequence of magnetic field swinging between negative and positive magnetic saturation.
- Demerit
  - This method takes a few tens of second to get one MO image.

MO imaging using LCM as polarization modulator

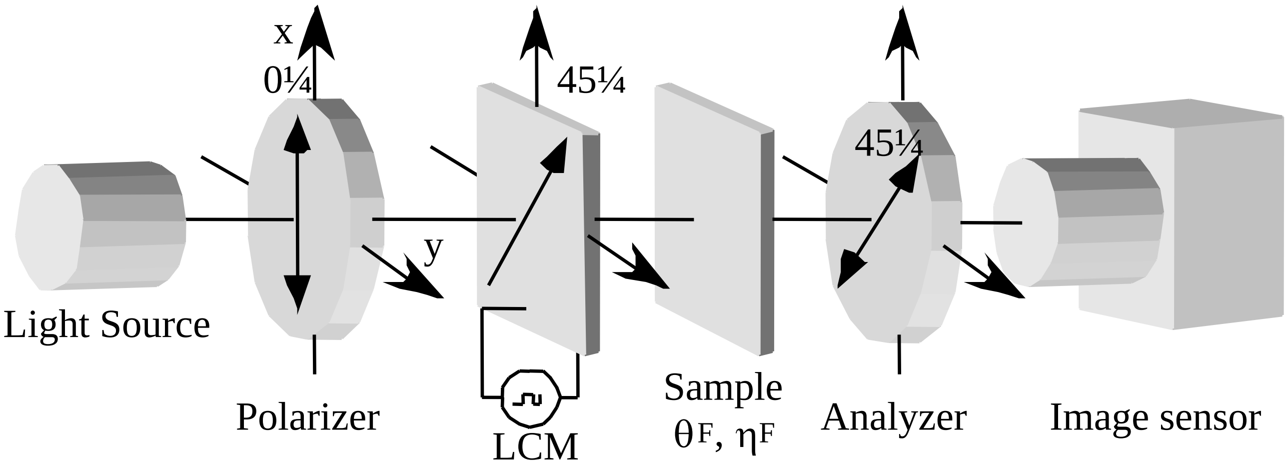

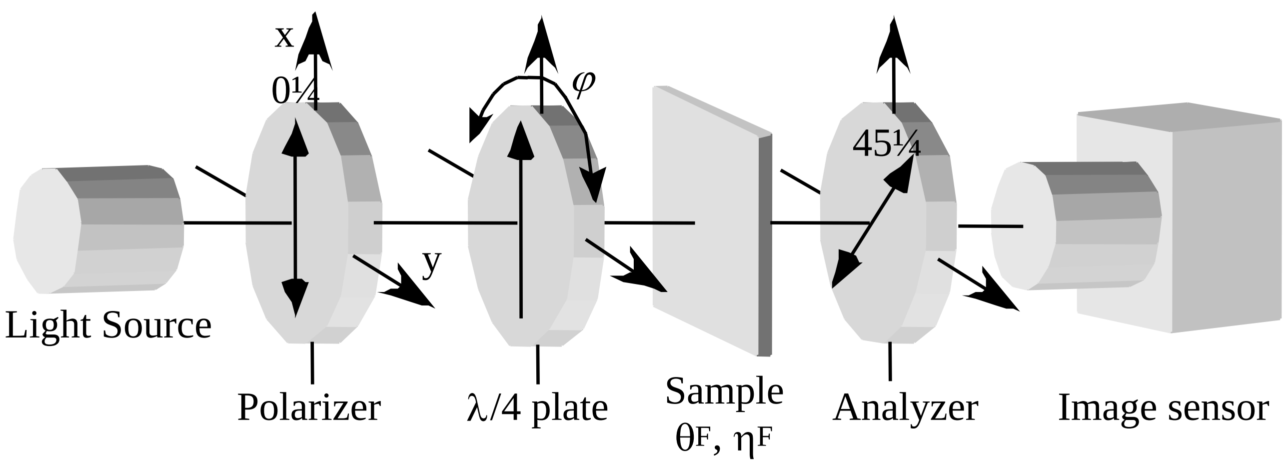

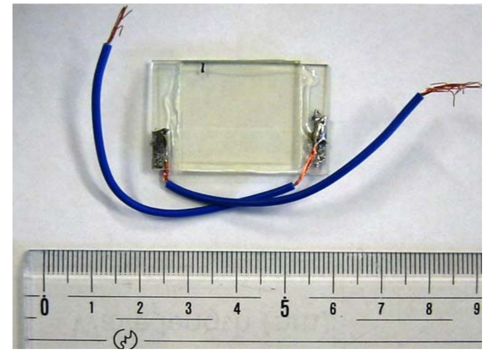

Liquid crystal: ZLI-4792
Substrate: ITO coated glass

T Ishibashi et al., J. Magn. Soc. Jpn. **4**, 278 (2004).
T Ishibashi et al., J. Appl. Phys. **100**, 093903 (2006).

MO microscope

CCD camera
- Hamamatsu C9300 201
- Number of Pixels 640 × 480
- Data transfer 150 frame/s

Computer
- CPU XEON 3.2GHz
- RAM 2GB

Interface
- AD-DA, GPIB, etc.

Software Development
- Visual Basic 6.0,
- Image capture SDK

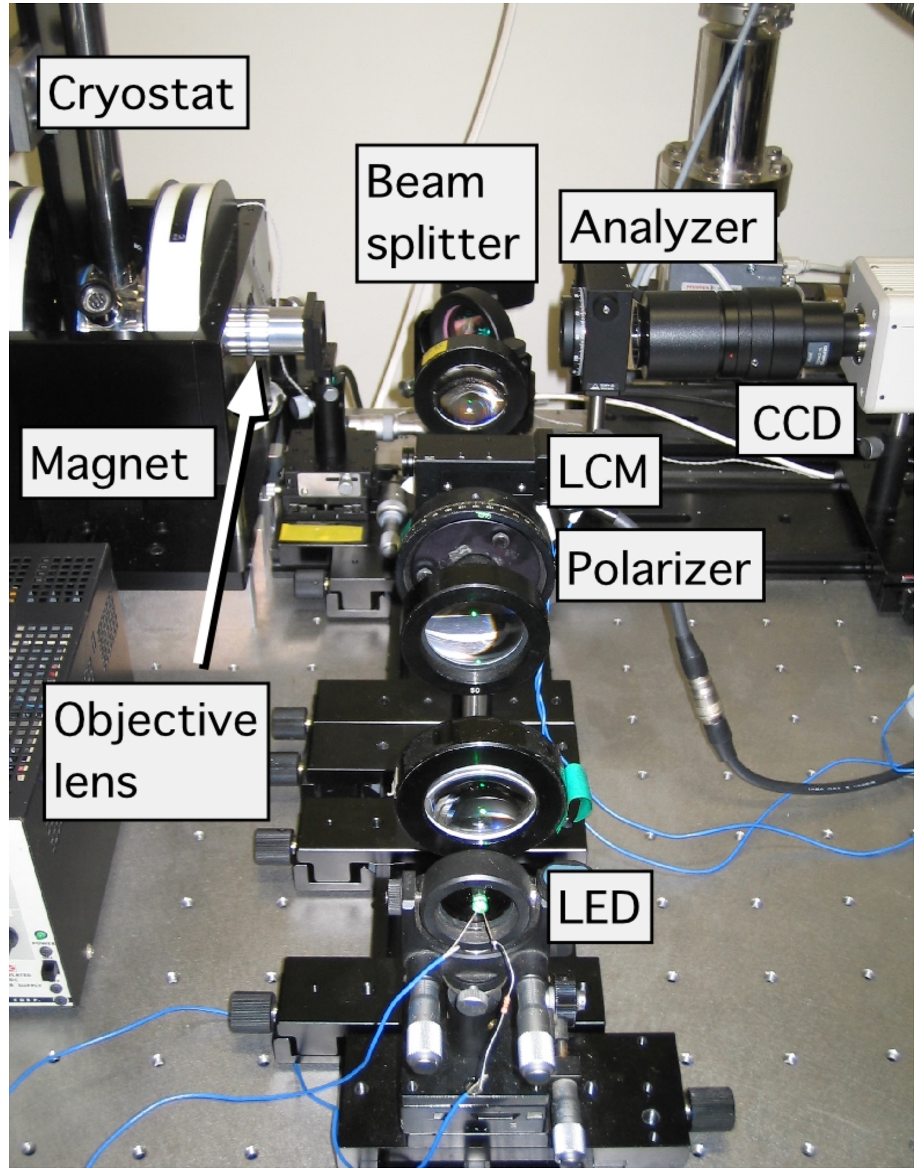

T ishibashi et al., JAP, 100, 093903 (2006).

Sequence of MO Measurement

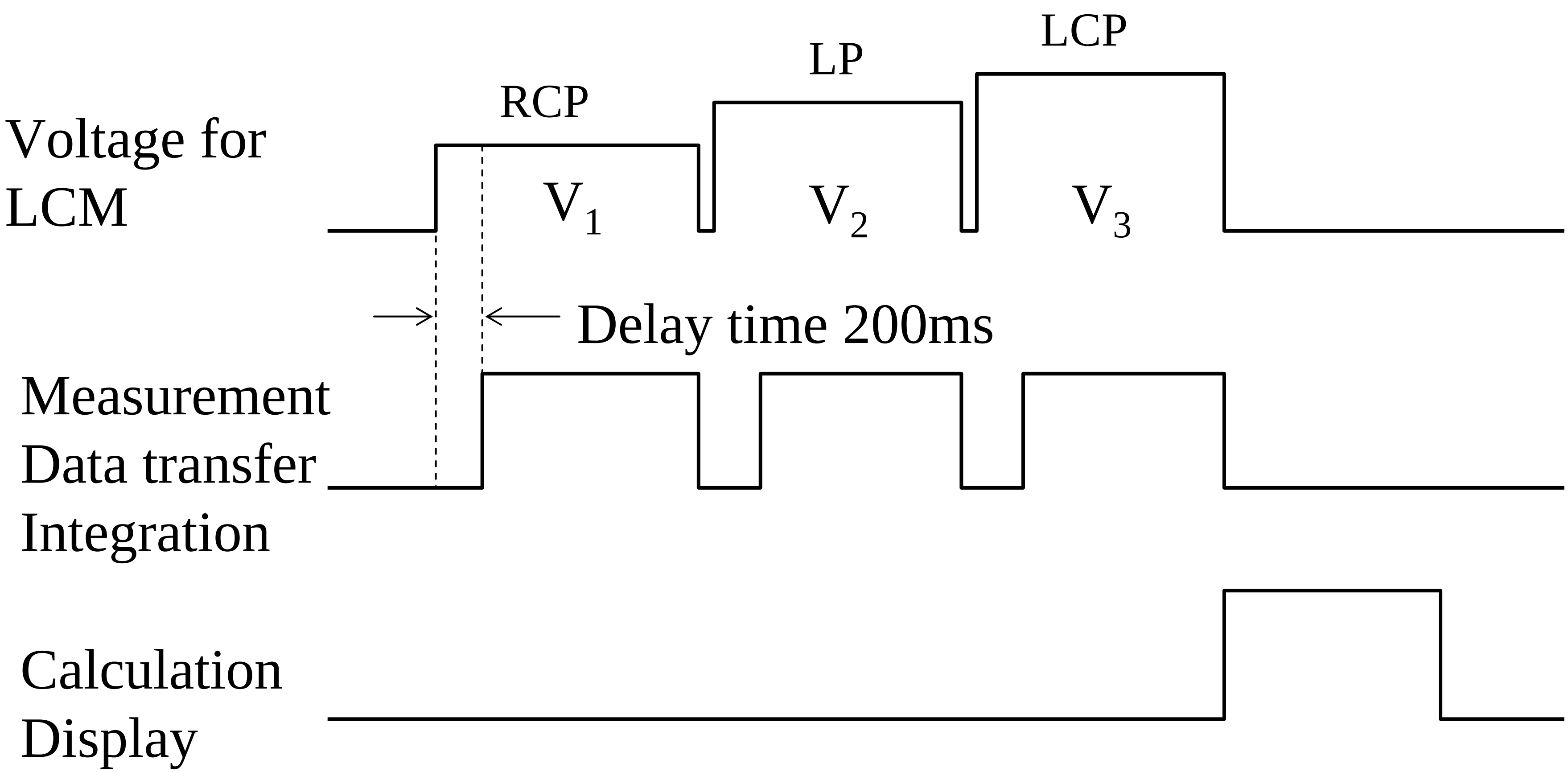

Real time observation

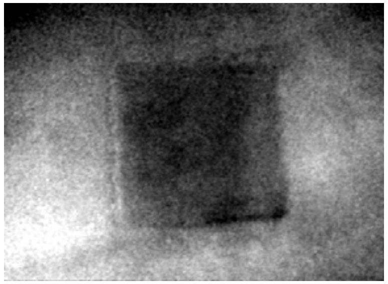
0s
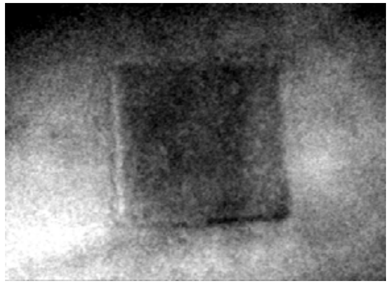
1s
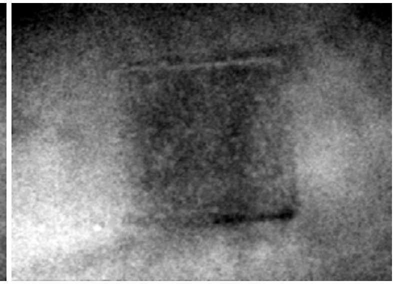
2s
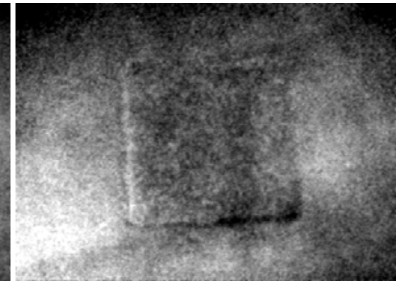
3s
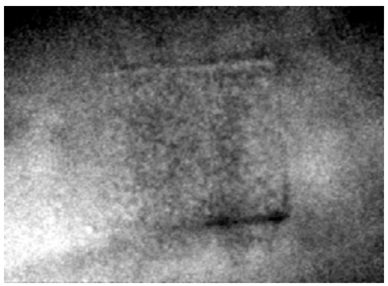
4s
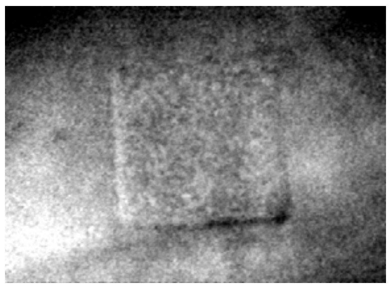
5s
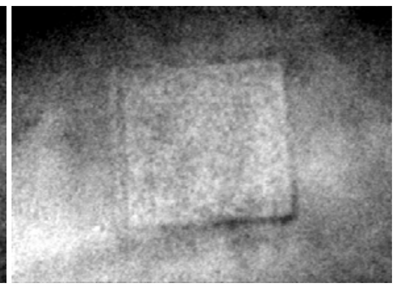
6s
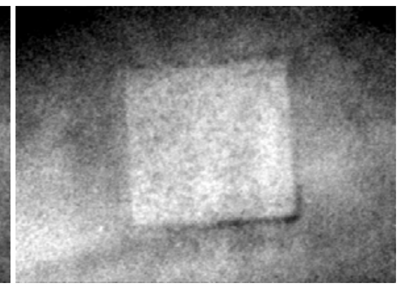
7s
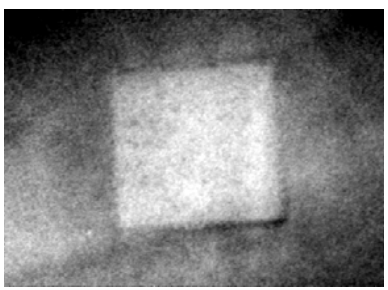
8s
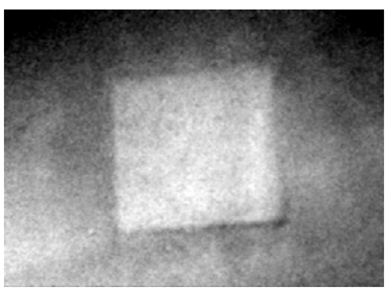
9s
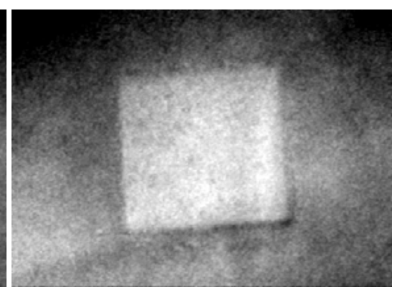
10s
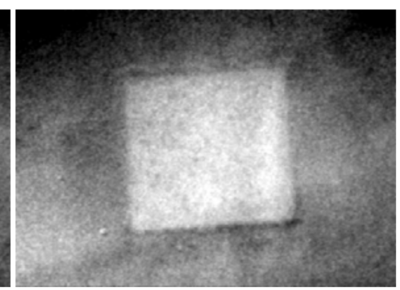
11s

Pattern size
50μm square

Sample
$Y_2BiFe_4GaO_{12}$

3. MO indicator film

Requirements for MO indicator

- Large Faraday effect

  For visualize magnetic field
- Thin film with a thickness of ~ 1μm

  To detect magnetic field near sample before its distribution smears out.
- In-plane magnetization without magnetic domain

  For high resolution magnetic image

Problem with Domain Structure

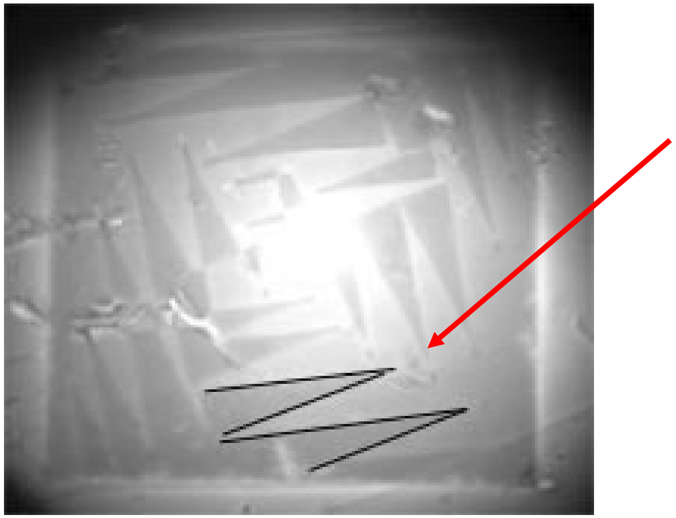

LPE grown garnet as indicator

If we use LPE garnet as an MO indicator, Zigzag-shaped magnetic domain appears in garnet film magnetized in-plane, which makes it difficult to observe a signal from a sample, especially in the case that a signal is small.

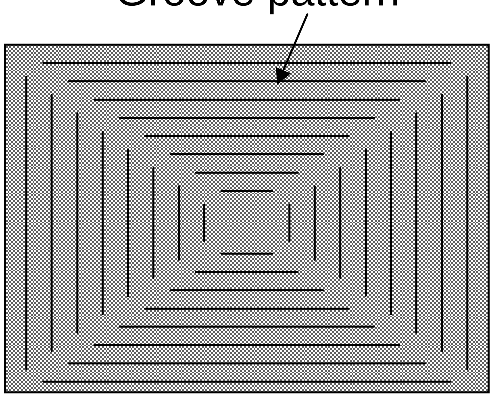

Nb film with groove pattern

MOD process

- MOD solutions (by Kojundo chemical lab.)
  made from carboxylic acids ~3 mol%
- Chemical compositions
  YBiFeO Y:Bi:Fe 2:1:5
- Sabstrate
  $Gd_3Ga_5O_{12}$ (111)

Cleaning of Substrates

↓

Spin Coating

Step1 500rpm 5sec

Step2 4000rpm 30sec

↓

Drying

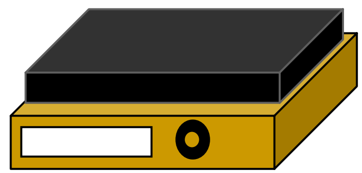

150℃ 5〜60min

↓

Pre annealing

450℃ 10min

↓

Crystallization

550℃〜900℃ 1h

Repeat

MO indicator film

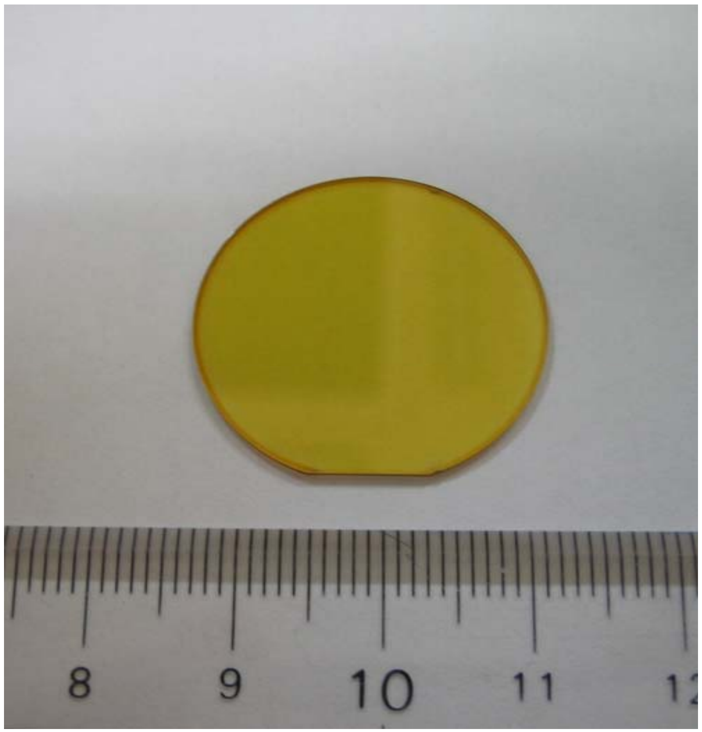

$Y_2BiFe_5O_{12}$/GGG(111)
Thickness 400 nm)

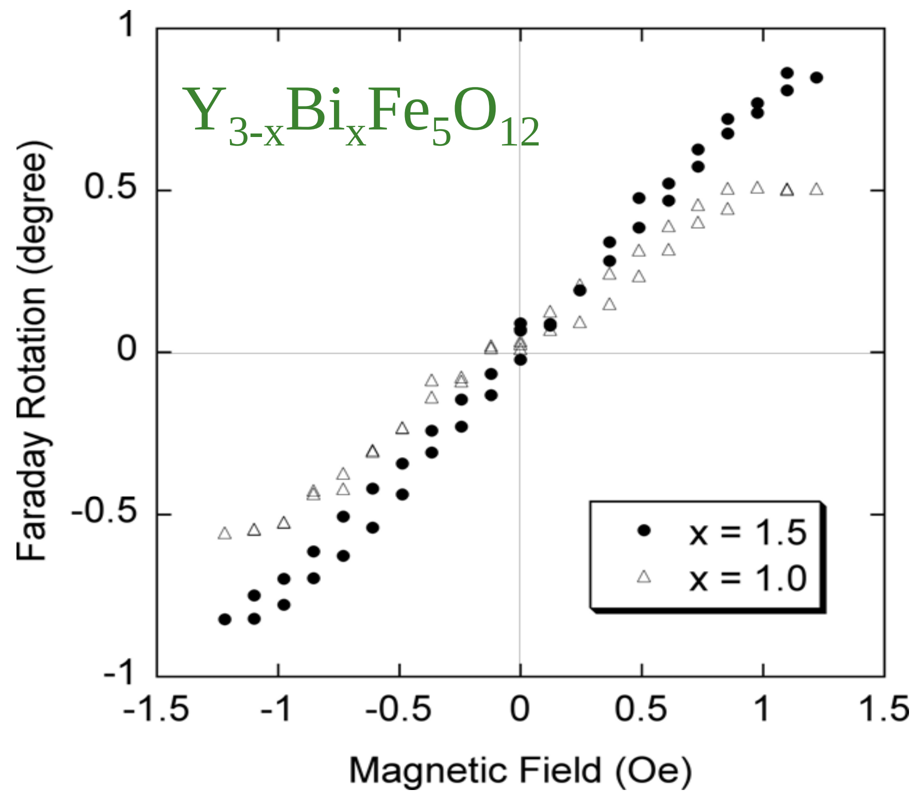

Magnetic field dependence of Faraday rotation

Problems are overcome with MOD indicator

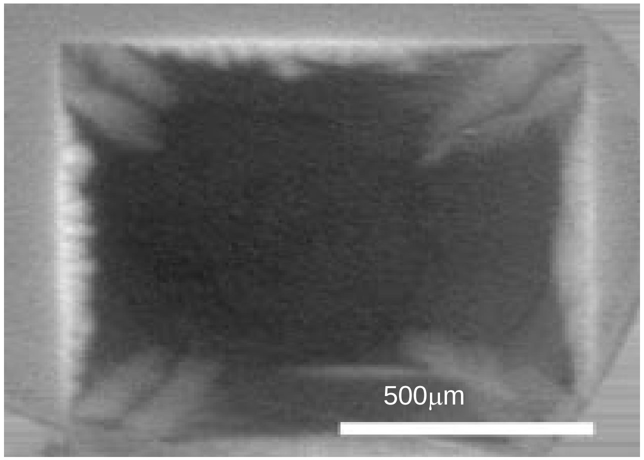

MOD grown garnet as indicator

Groove pattern

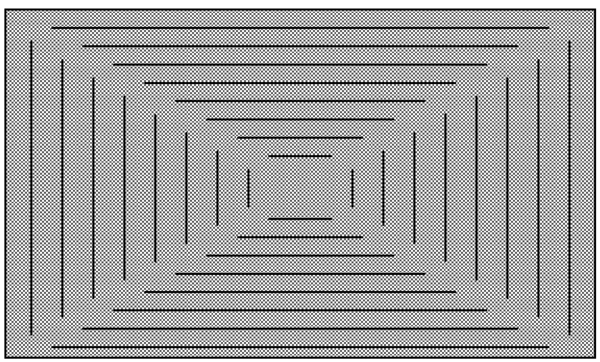

Nb film with groove pattern

MO indicator films without visible magnetic domain structure prepared by MOD (metal-organic decomposition) Is suited for observation of small signal from the sample.

4. Magnetic imaging

(1) Superconducting film

Sample setups

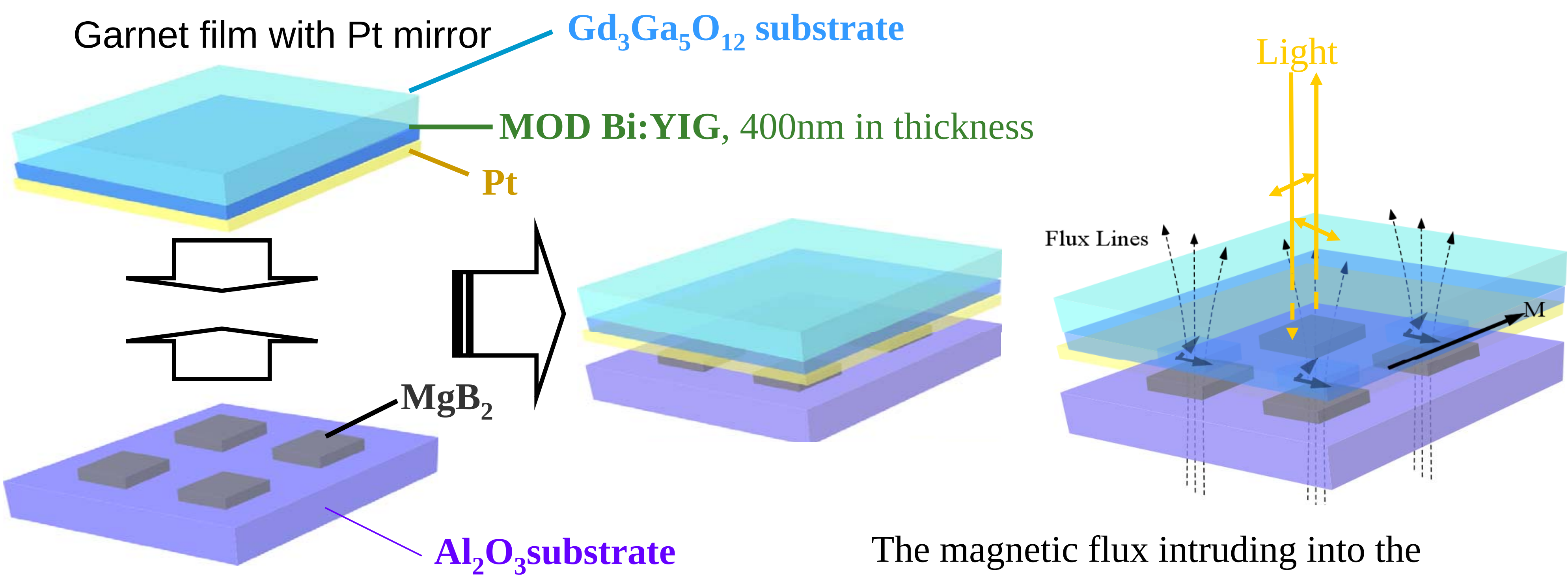

MgB_2 pattern

Prepared by MBE
Patterned by photolithography
thickness:100nm
T_c～30K

The magnetic flux intruding into the superconductor is transferred to the indicator film, The perpendicular component of the magnetization is observed by Faraday effect.

Magneto-optical image

Patterned MgB_2 film

Grown by NTT research lab.

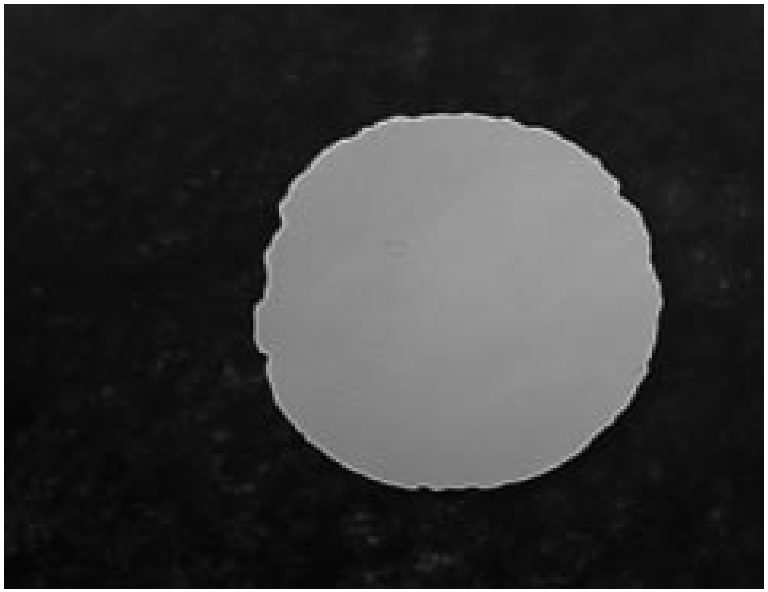

0.3 mm

Circle pattern
Diameter: 0.5mm

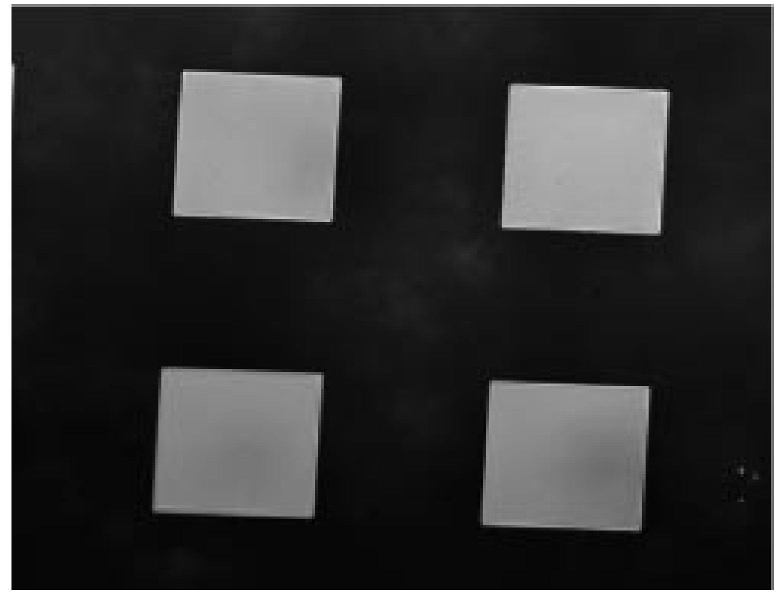

100μm

Square pattern
Size: 100μm × 100μm

Optical images

The image from the indicator side prevents direct optical image of circular dot due to Pt-mirror.

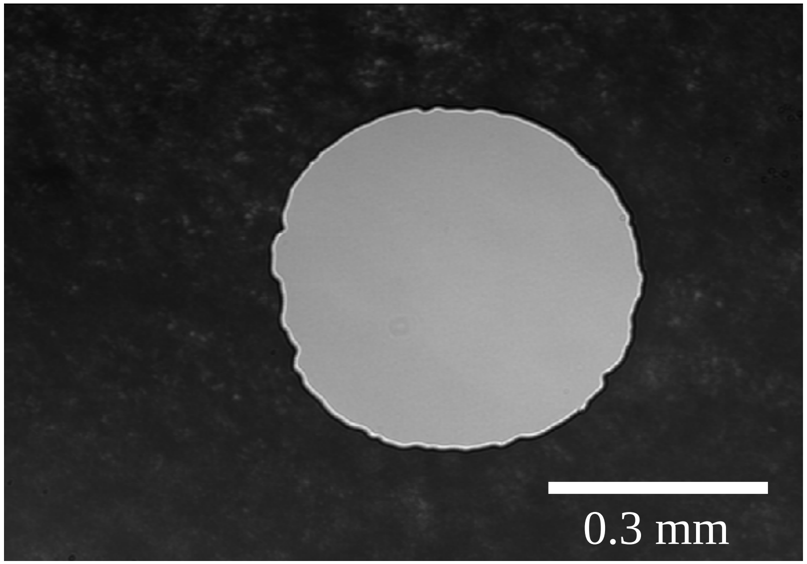

Optical image (×5) of MgB_2 pattern(0.5mm ϕ)

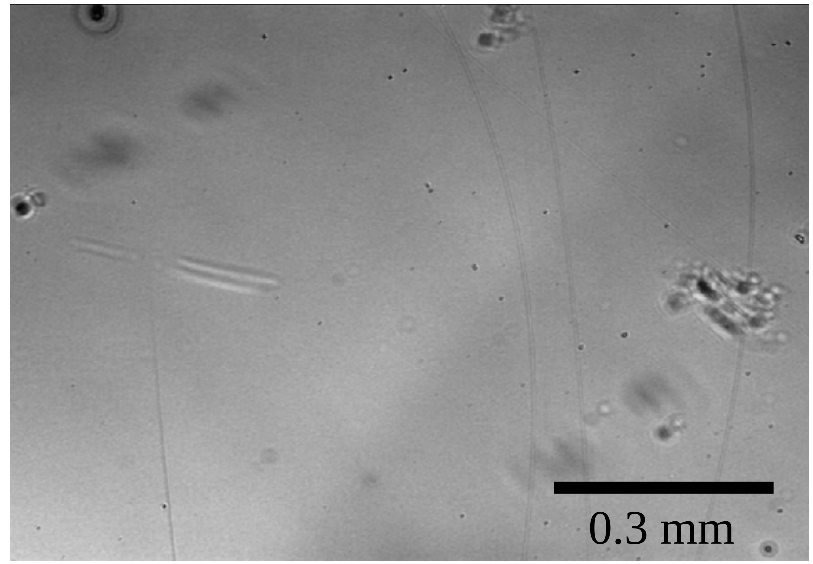

Optical image (×5) from indicator

No direct optical image of MgB_2 pattern is observed due to Pt mirror.

⇩

Only the magnetic fluxes can be visualized.

The image from the indicator side prevents direct optical image of square dots due to Pt-mirror.

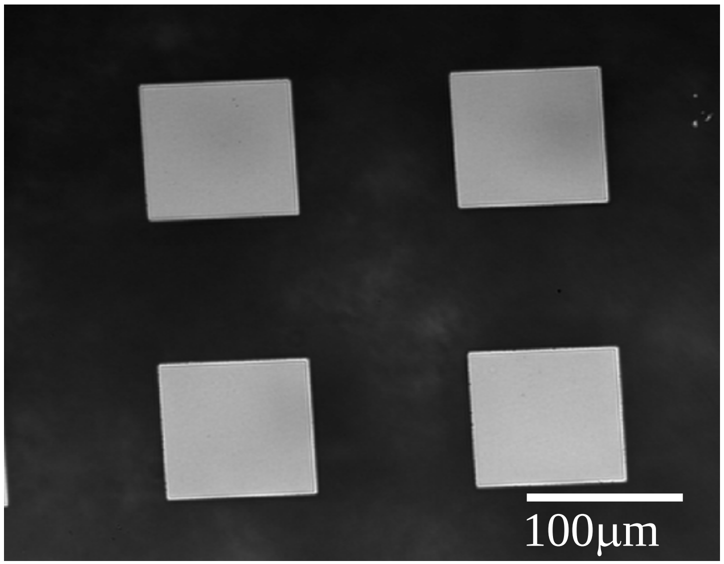

Optical image (×10) of MgB_2 square dots(100μm×100μm)

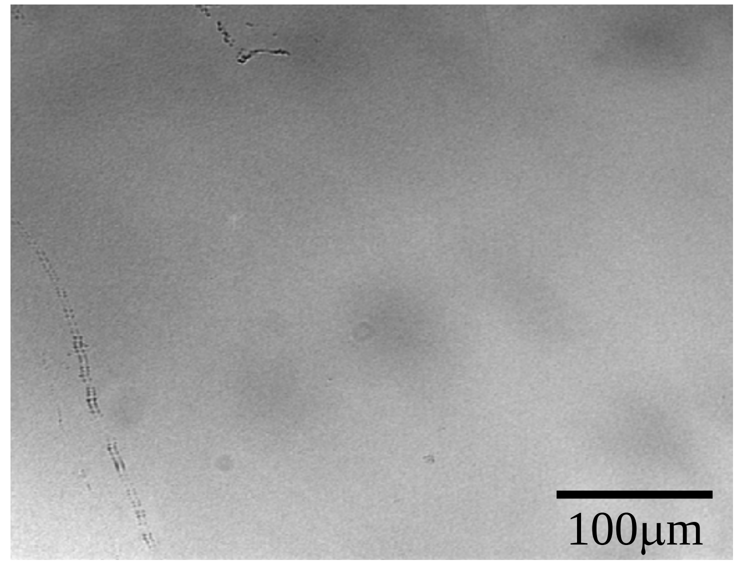

Optical image (×10) after stacking with the indicator.

MO images of 500μm circle

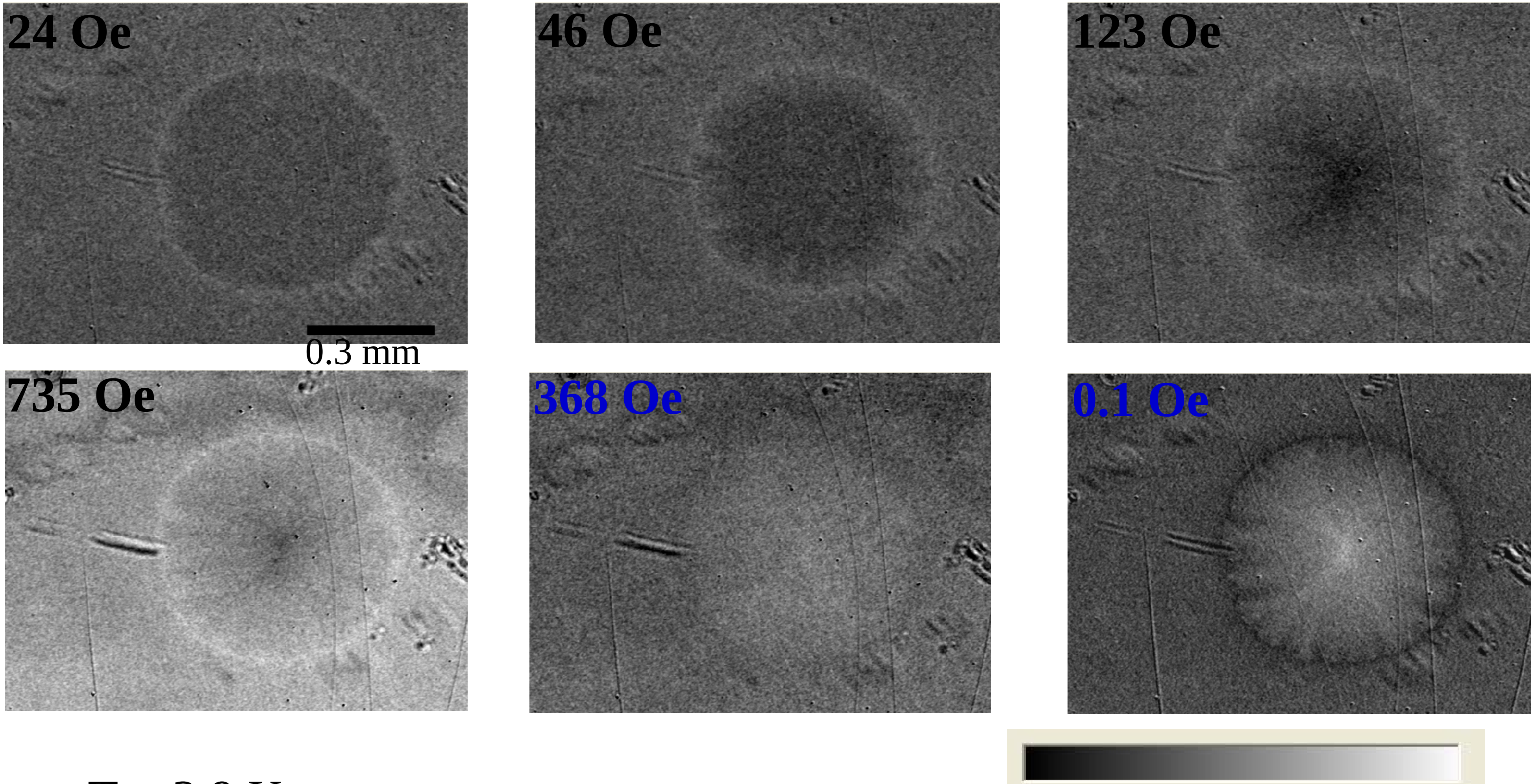

T = 3.9 K

MO images showing intrusion of magnetic fluxes into an MgB_2 circular dot at T=3.9K.

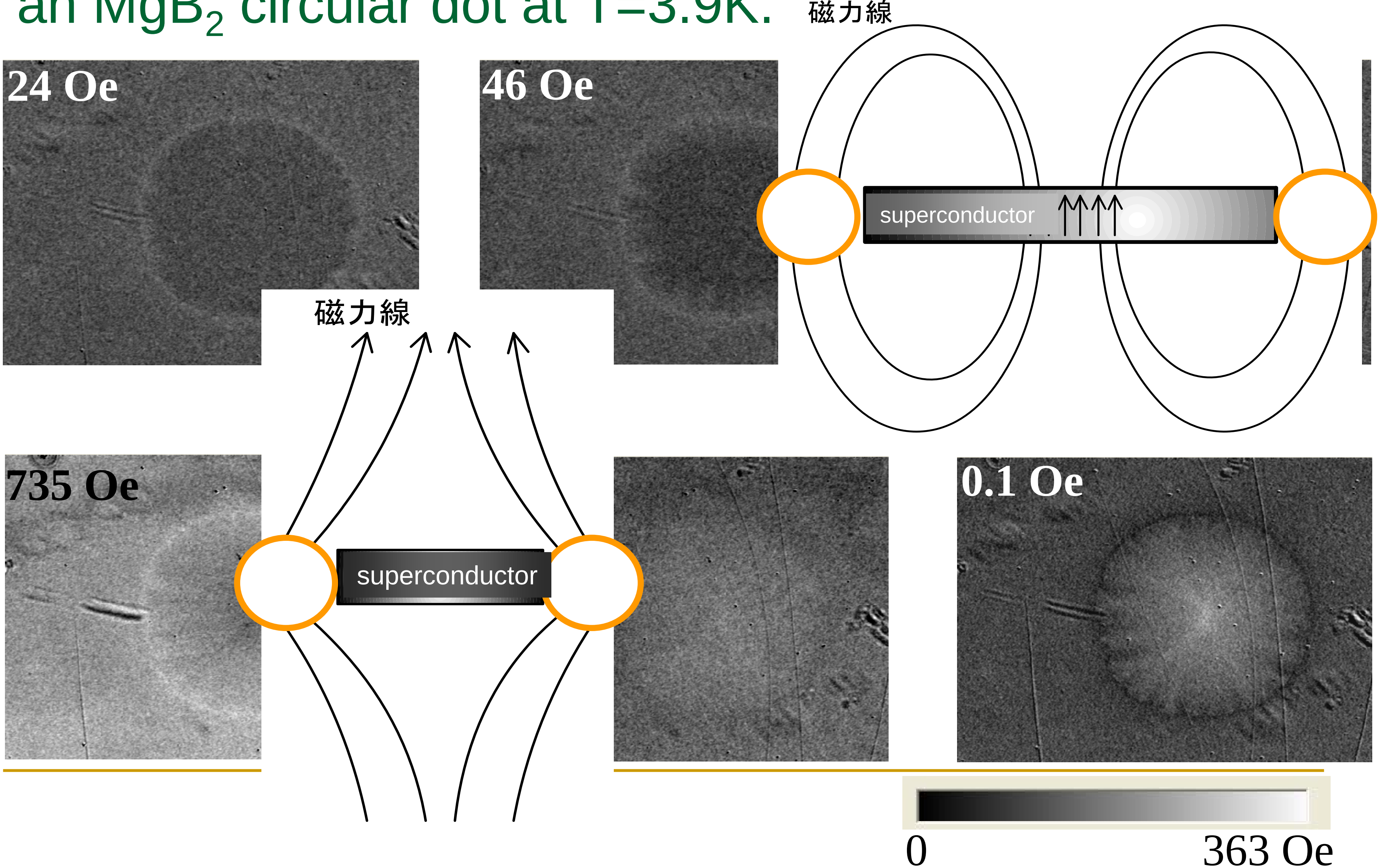

MO images of 100µm square

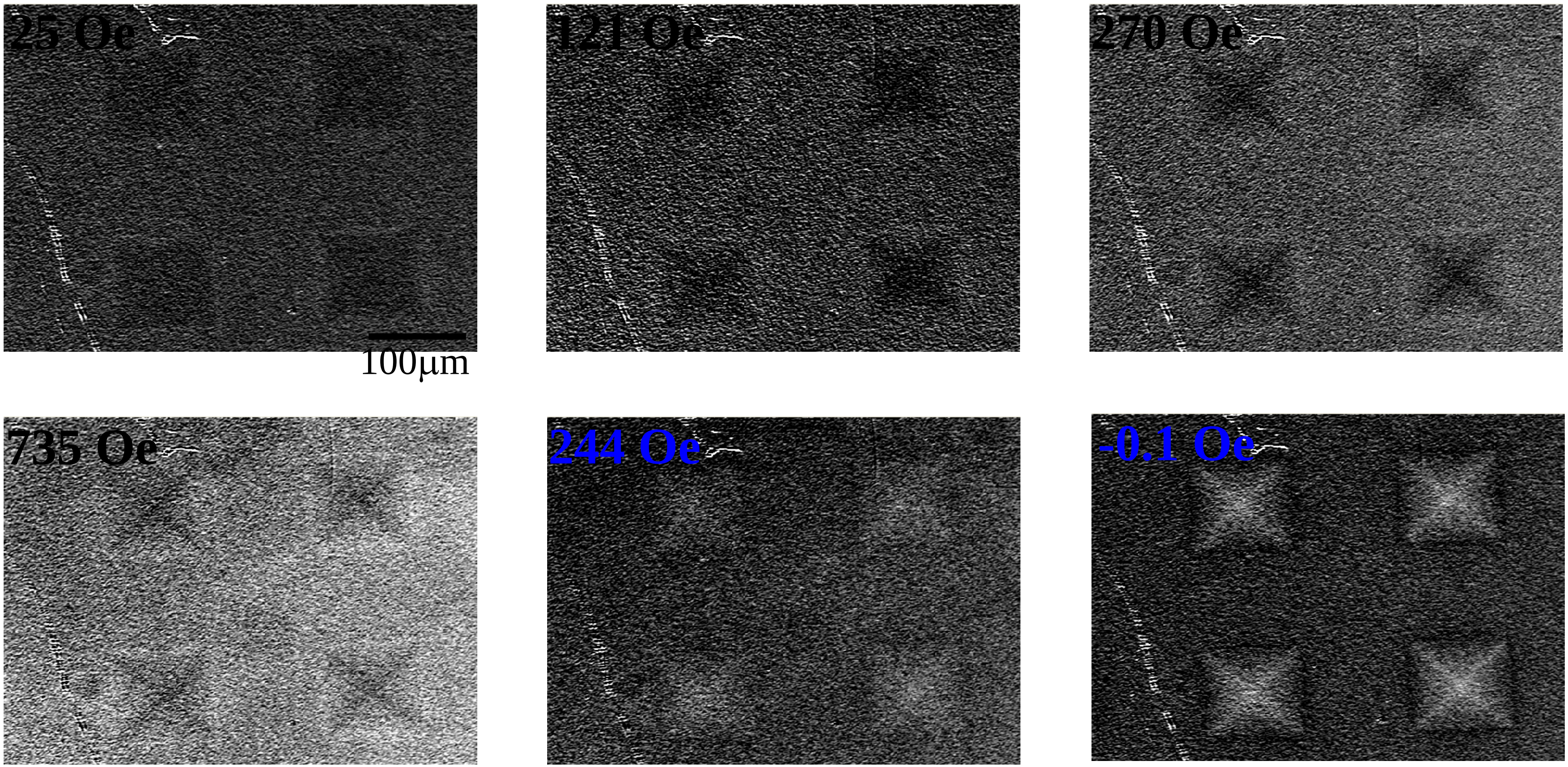

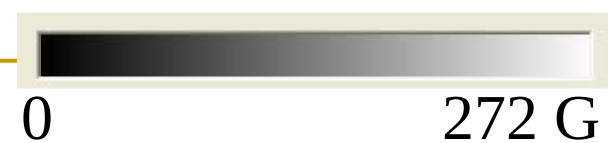

T=3.9K

Magnetic image

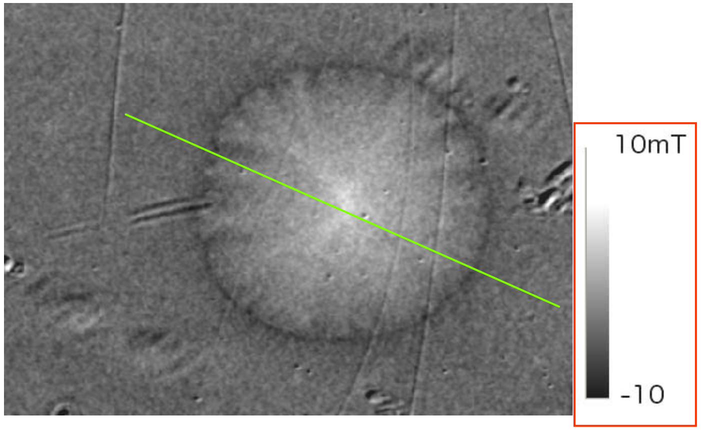

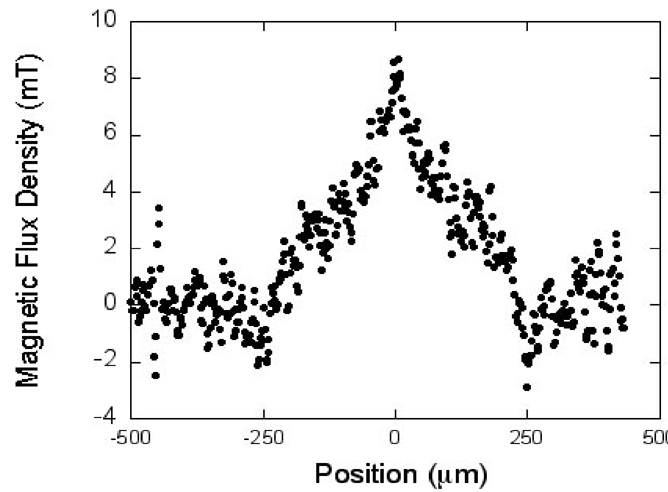

Magnetic image of remanent state after application of Magnetic field of 735 Oe.

Quantitative magnetic image can be obtained from MO image by using linear relation θ_F- B for the MO indicator film.
Therefore, contrast in the image directly shows a magnetic field, B.

MO image of MgB_2

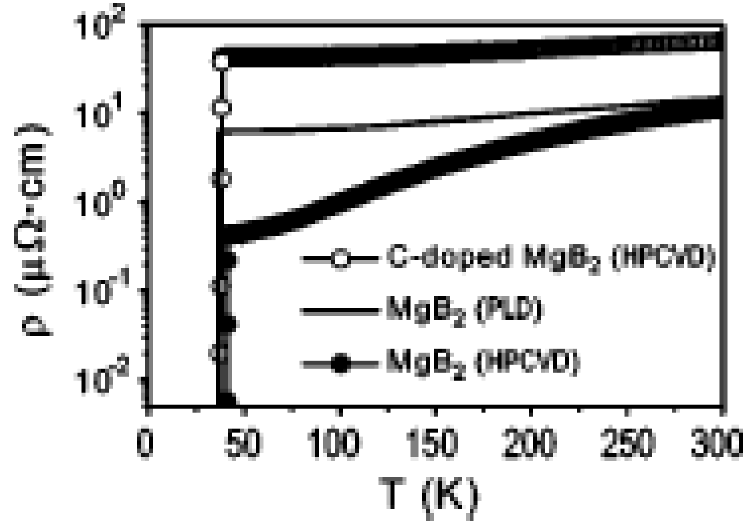

FIG. 4. Temperature dependence of resistivity of the C-doped and ultrapure MgB_2 films plotted along with the pure MgB_2 film made by PLD (Refs. 5 and 16).

Z. X. Ye et al., APL 85 (2004) 5284.

MBE-grown MgB_2

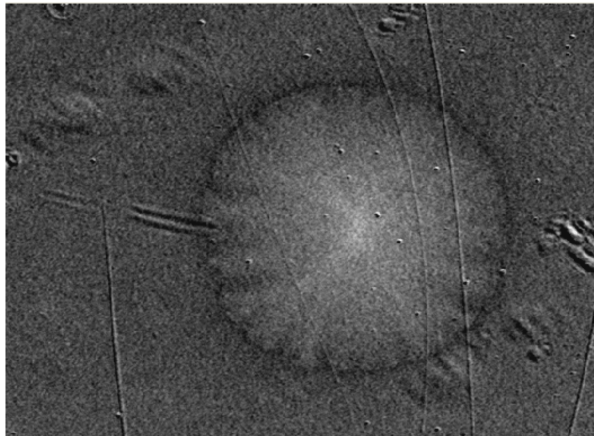

Present work

PLD-grown MgB_2

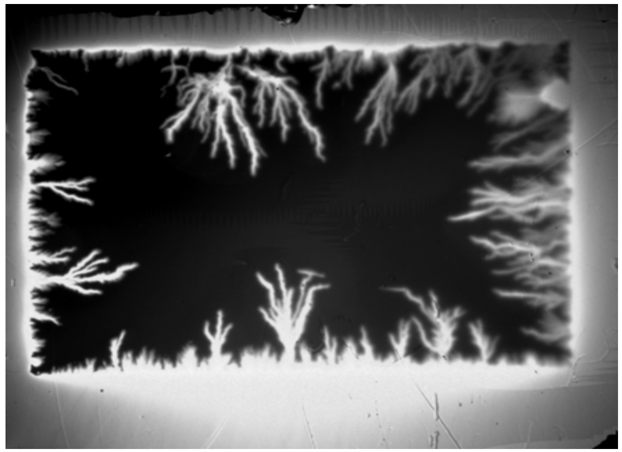

Oslo University

How to obtain current distribution from MO images

- Ampére's law

$$\mu_0 \boldsymbol{J} = \Delta \times \boldsymbol{B}$$

It needs all B component, Bx, By, Bz, while MO images measures only Bz.

- Biot-Savart's law

$$B_z = \frac{\mu_0}{4\pi} \int \frac{(\boldsymbol{y} - \boldsymbol{y}')J_x - (x - x')J_y}{\left|\boldsymbol{r} - \boldsymbol{r}'\right|^3} dx'dy'$$

1) One uses models for current distribution and compare the calculated B with the measured one.
2) One directly inverts by numerical method.

Inversion of Biot-Savart's law using convolution theorem

Ch. Jooss et al. Physica C,299(1998)215.

$$\boldsymbol{B}_z = \mu_0 H_{ex} + \mu_0 \int_V K_g(\mathbf{r},\mathbf{r}')g(x,y)d^3r' \quad \cdots \ (1)$$

g : local magnetizaion

K_g : green function

z component of magnetic dipole

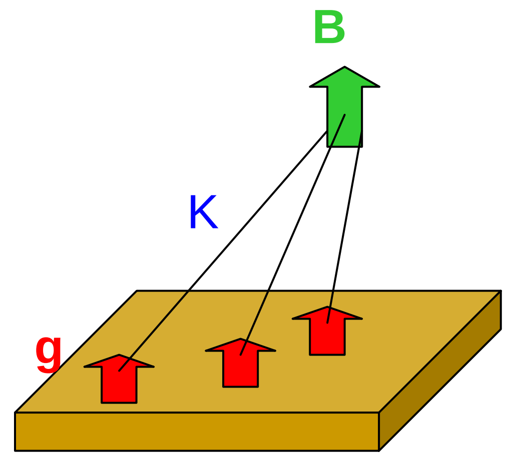

Using convolution theorem

Eq.(1) can be transformed into

$$\tilde{\boldsymbol{B}}_z(\boldsymbol{k}) = \mu_0 \tilde{K}_g(\boldsymbol{k})\tilde{g}(\boldsymbol{k})$$

x and y component of J are obtained as

$$\Delta \cdot \boldsymbol{J} = 0$$

$$\tilde{j}_x = -i\frac{\tilde{\boldsymbol{B}}_z}{\tilde{K}_x} \qquad \tilde{j}_x = -\tilde{j}_x \frac{k_x}{k_y} \qquad \tilde{K}_x = \mu_0 \frac{e^{-kh}}{k} sinh\left(\frac{kd}{2}\right)\left[\frac{k_y}{k} + \frac{k_x^{\,2}}{k_y k}\right]$$

Magnetic & Current images

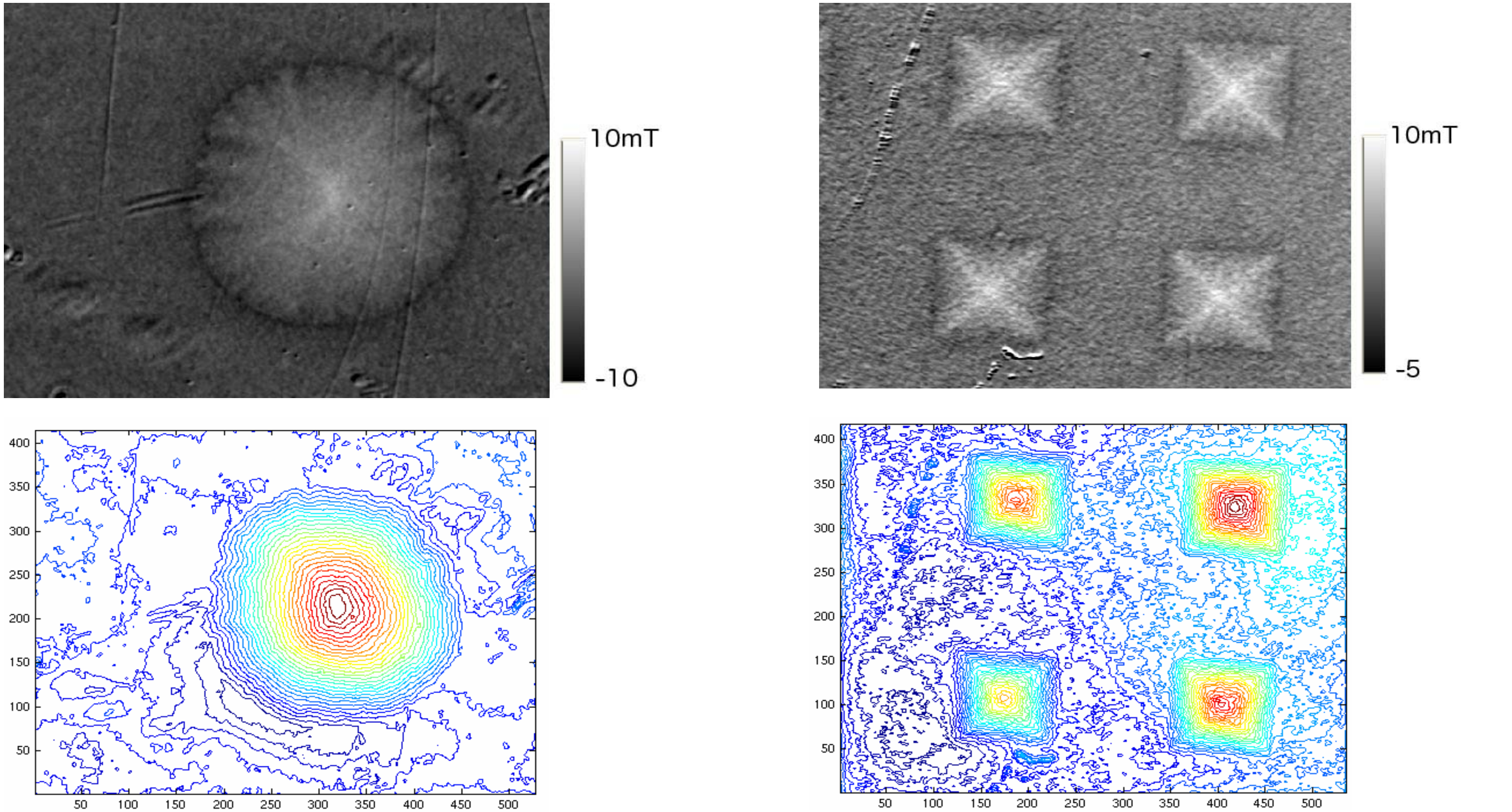

Density of lines corresponds to current density.

Color indicates local moment obtained in a calculation.

Current density ~ $6 \times 10^7 A/cm^2$

Nb pattern prepared on Bi:YIG

- Substrate $Gd_3Ga_5O_{12}$(111)
- MO indicator film

  $Y_2BiFe_5O_{12}$ (400nm)

  by MOD mothod
- Superconductor

  Nb (150nm)

  by sputtering method
- Mirror Au
- Pattern size of anti-dots

  7, 10, 15μm□

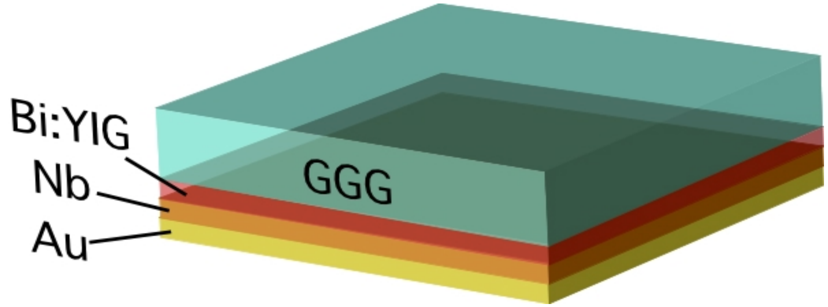

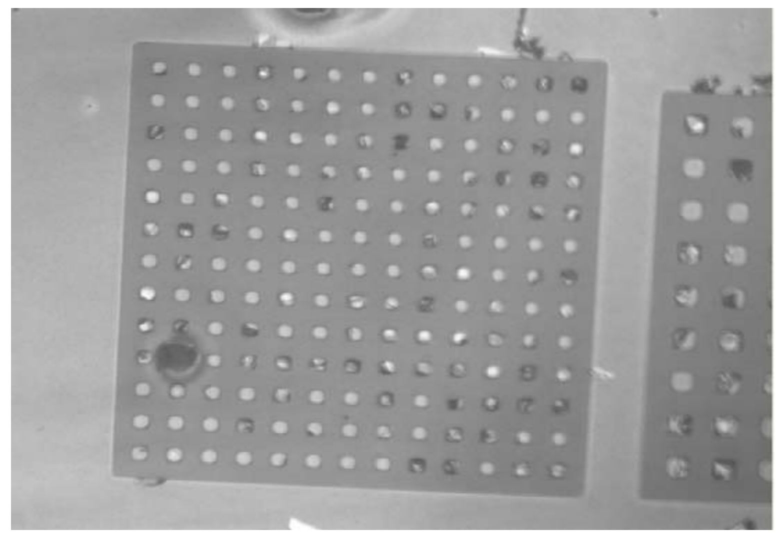

Optical image

MO images of 10mm anti-dots

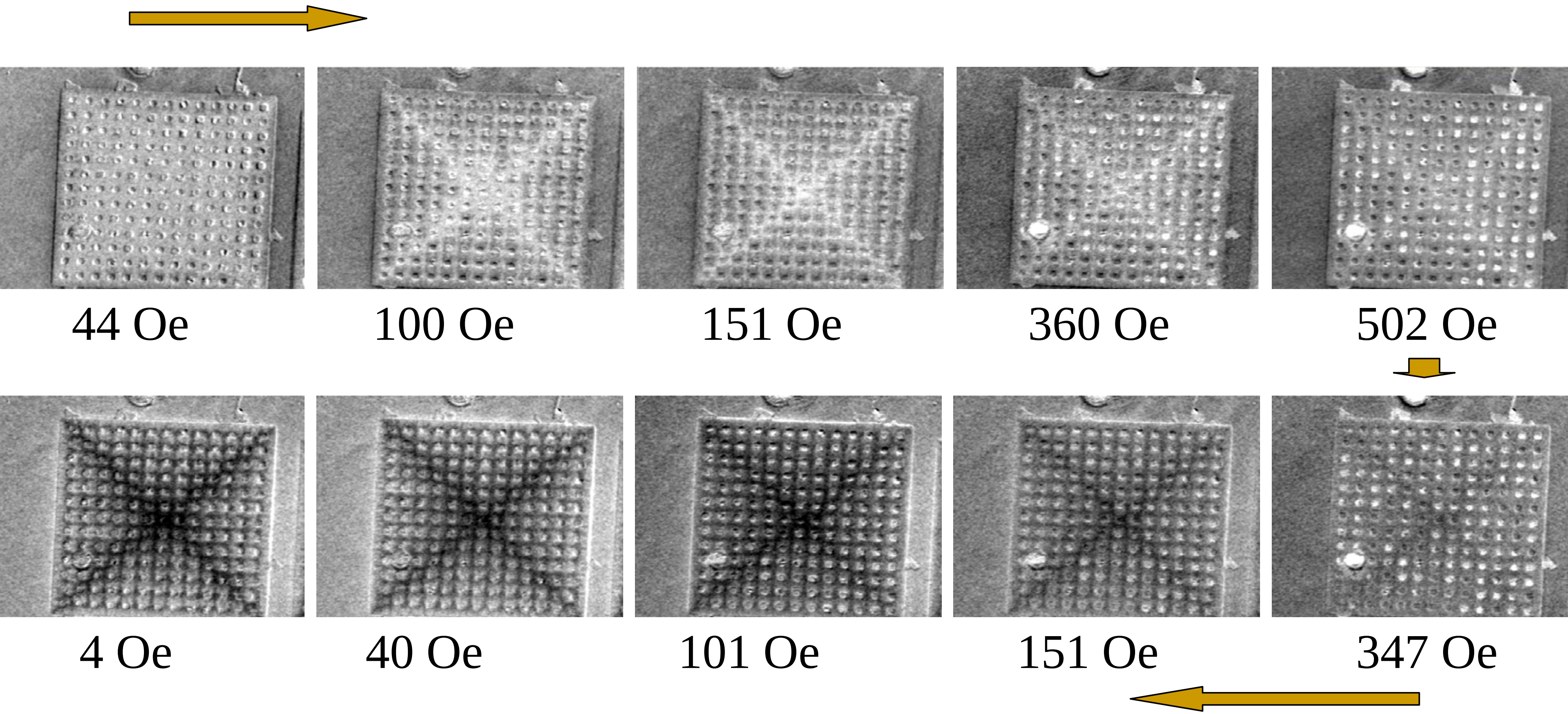

MO images of Nb 10μm × 10μm anti-dots pattern with applying magnetic field. The sample was zero-field cooled down to 3.5K.

High resolution MO image

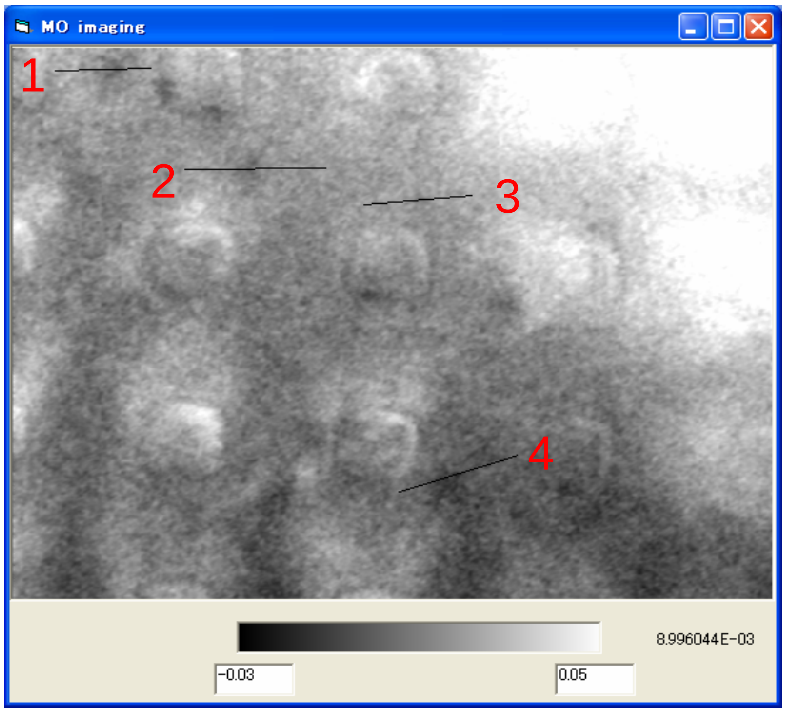

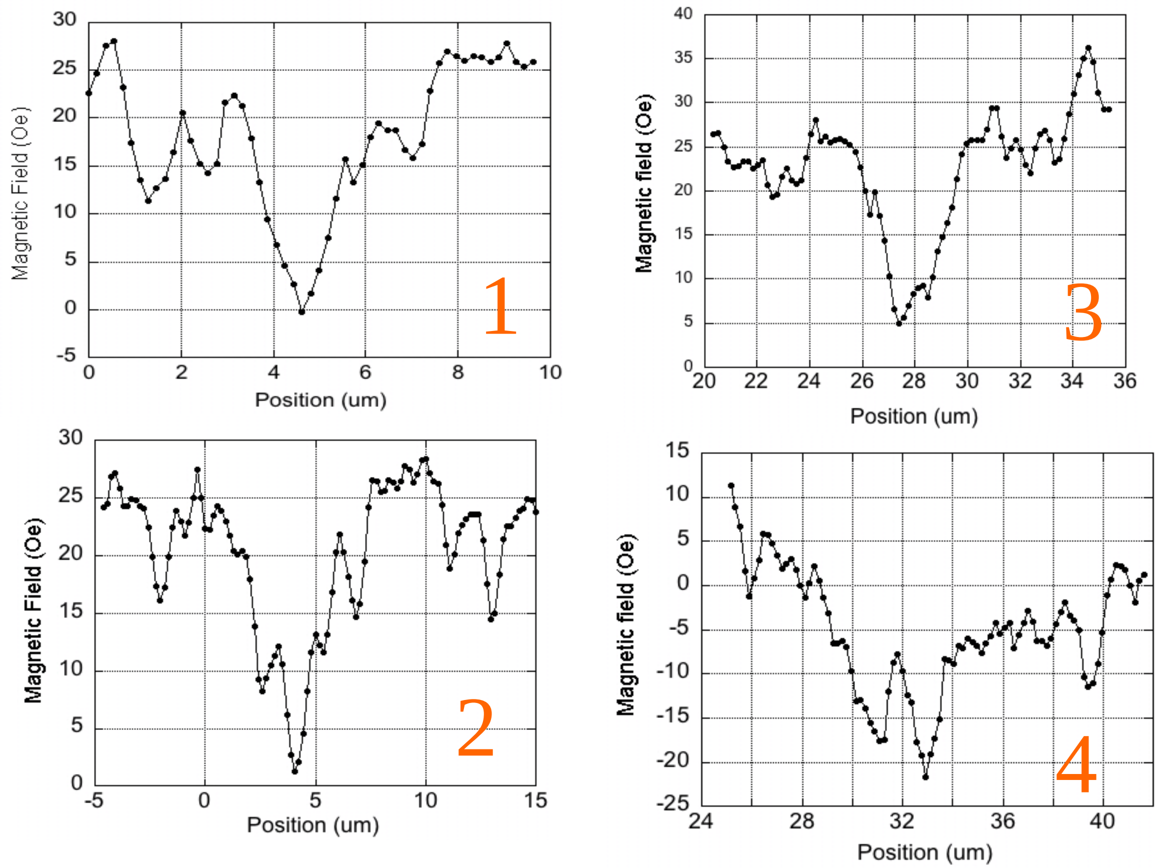

4. Magnetic imaging
(2) Magnetic structures

Y-shaped patterns buried in Si

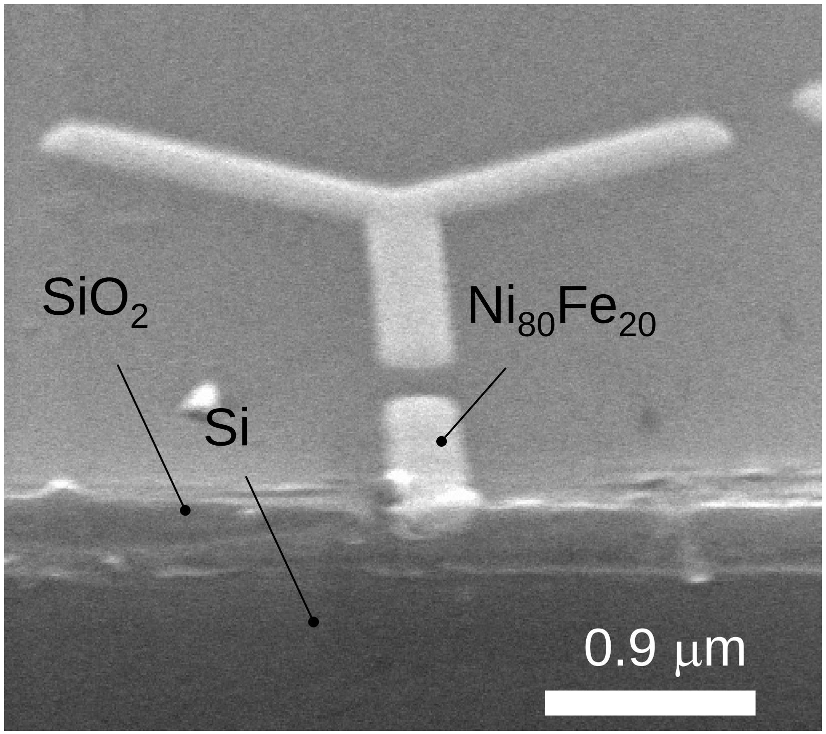

Cross sectional SEM image

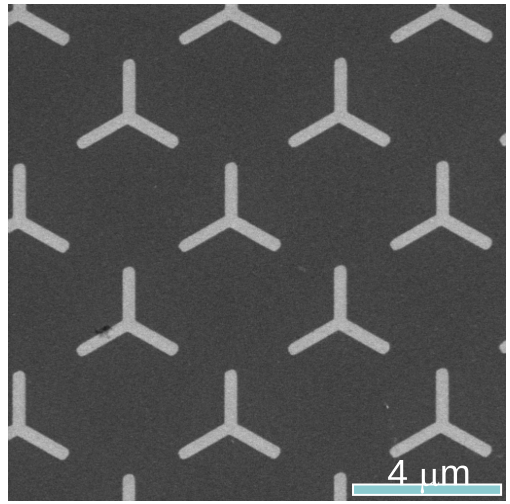

Linearly aligned

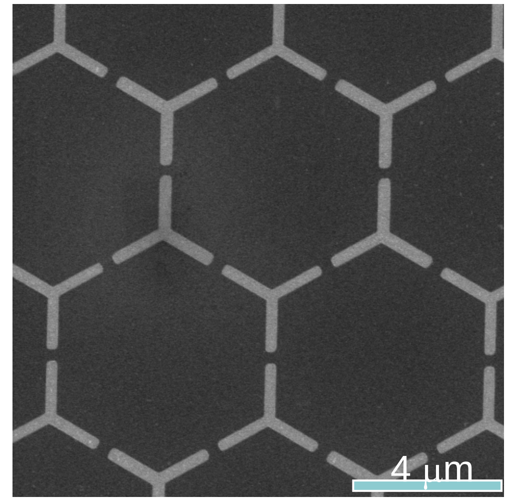

Honeycomb aligned

MO Observation of Y-shaped patterns

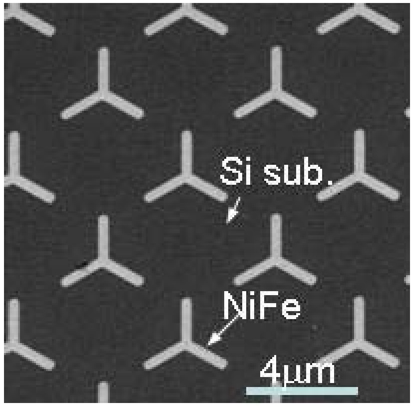

SEM image

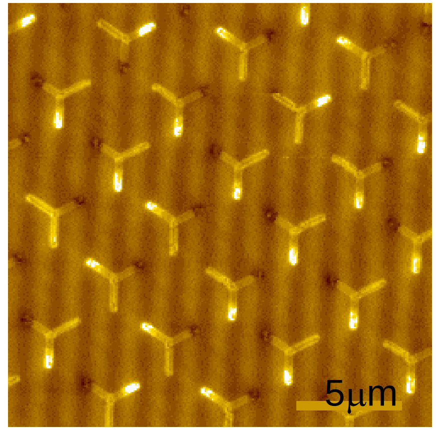

MFM image

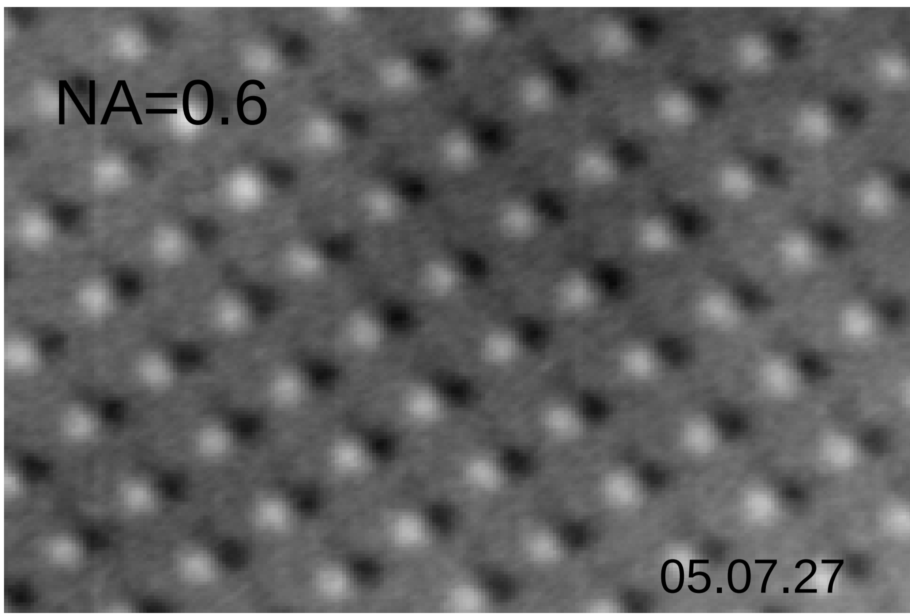

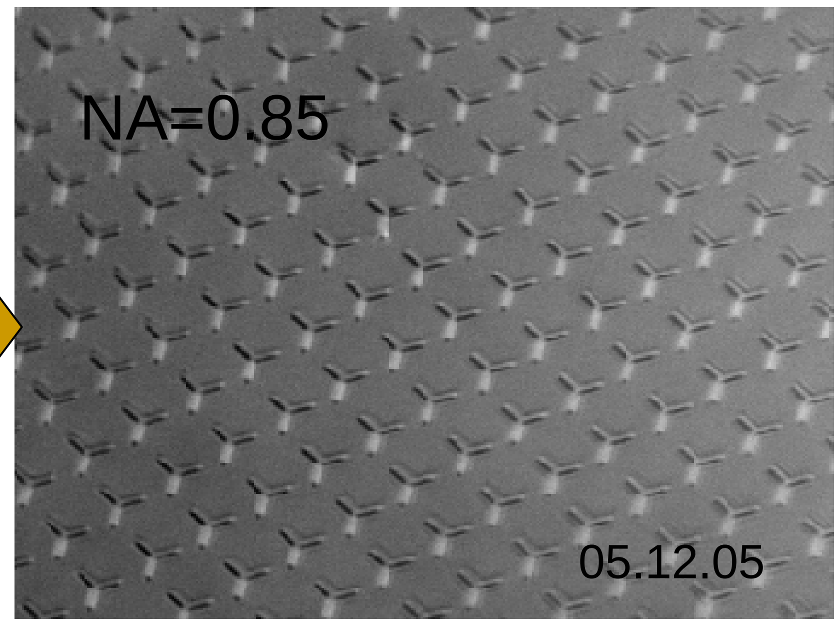

MO images

Use of MO indicator for observation of in-plane magnetization

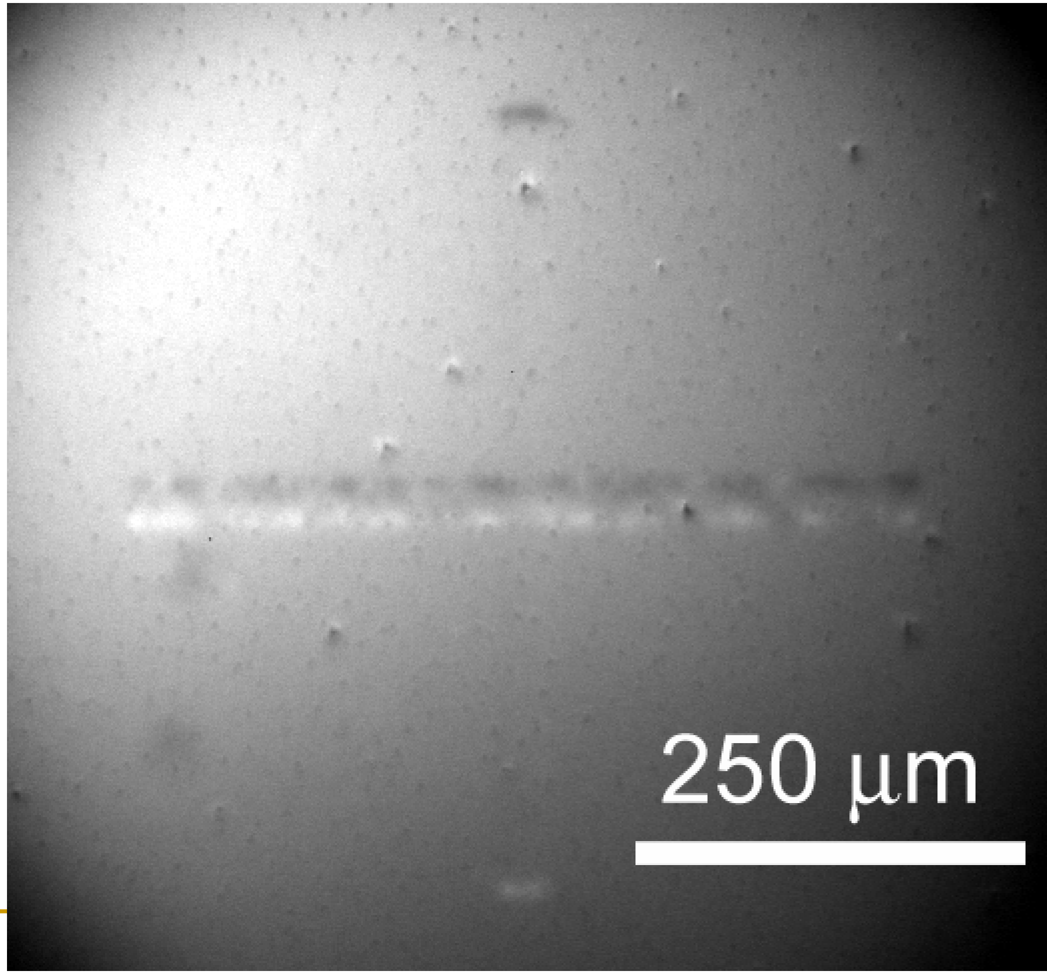

Conclusions

- Quantitative magnetic imaging by the MO imaging technique using the polarization modulation technique combined with MO indicator films was developed.
- This technique allows us quantitative and nondestructive measurements for magnetic stray field as well as current distribution.
- Evaluations of stray field, current distribution were demonstrated for the superconducting MgB_2 patterned sample.

Acknowledgement

This work has been supported in part by the Grant-in-Aid for Scientific Research (No.16360003) from the Japan Society for Promotion of Science. We thank Dr. H. Shibata of NTT basic Research Laboratory and Prof. M. Naito of Tokyo Univ. of Agriculture and Technology for MgB_2 sample. We also thank Prof. T. H. Johansen and Mr. J. I. Vestgården of Univ. of Oslo for calculation of current images.

Prof. M. Naito

Prof. T. H. Johansen

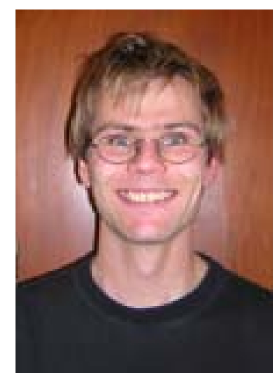

Mr. J. I. Vestgården